8-14-2013 12:00 AM

Oil-in-water Emulsification Using Oscillatory Micro-screen

Jiangshan Liu, *The University of Western Ontario*

Supervisor: Dr. Hassan Gomaa, *The University of Western Ontario*
Joint Supervisor: Dr. Jesse Zhu, *The University of Western Ontario*
A thesis submitted in partial fulfillment of the requirements for the Master of Engineering
Science degree in Chemical and Biochemical Engineering
© Jiangshan Liu 2013

OIL-IN-WATER EMULSIFICATION
USING OSCILLATORY MICRO-SCREEN

(Thesis format: Monograph)

by

Jiangshan <u>Liu</u>

Graduate Program in Chemical and Biochemical Engineering

A thesis submitted in partial fulfillment
of the requirements for the degree of
Master of Engineering Science

The School of Graduate and Postdoctoral Studies
The University of Western Ontario
London, Ontario, Canada

Abstract

A novel emulsification technique has been developed for high throughput production of uniform emulsion droplets using high porosity oscillating stainless steel wire woven micro-screen. Different surfactants were investigated including dispersed/continuous bi-surfactant systems using Span80/SDS and Span80/Tween20. The effects of oscillation amplitude and frequency as well as the dispersed phase flux on emulsion average droplet size and uniformity were investigated. It was found that the droplet average size decreased with increasing the surface sheer stress. The emulsion droplet uniformity determined using the coefficient of variation (CV) changed with oscillations such that there was an optimal oscillating frequency for each amplitude where the CV was smallest. Furthermore, it was also found that both droplet size and uniformity were influenced by the content of surfactants and that the effect of process conditions was stronger for Span80/SDS system than for Span80/Tween20 system. The experimental data were fitted satisfactorily using shear stress function with R^2 value of 0.97. Inserts were used to narrow the width of the continuous phase container and to build geometric channels. The flat surface inserts, the wavy surface inserts and the inserts with baffles have been studied. The results show that the droplet size decreased and the size distribution was widened. In the respect of monodispersion, the continuous phase channels with various geometries have detrimental influences in the oscillatory micro-screen emulsification system.

Keywords

Acknowledgments

I would like to express my great gratitude to my supervisors, Dr. Hassan. G. Gomaa and Dr. Jesse Zhu. Thanks for their correct guidance, useful comments and fruitful discussion through the learning process of this master thesis. Furthermore, I also appreciate the trust, patience and encouragement which my supervisors offered to me. These all convey me a spirit of adventure in regard to research. Without their persistent help, this thesis would not have been possible.

Much appreciation is extended to my sincere colleagues and friends, Dr. Zhang Hui, Dr. Liu Yong, Dr. Song Long, Danni Bao, Jing Fu, Shan Gao, Chengxiu Wang and George Zhang. So many people have helped me in the first year since I've been in Canada. Thank them for helping me engage the Canadian culture and bring a lot fun to my life. In addition, I am grateful for their valued assistances and suggestions in the research and writing of this thesis. Their kindness touched me and gave me a thankful heart for the world.

My deepest gratitude goes to my beloved mother and father. I sincerely thank for their love, understanding and encouragement. Without their support, I could not be the one what I am today. With their company, I can keep moving forward without hesitation in the future.

Table of Contents

List of Tables

List of Figures

Nomenclature

a	Oscillating amplitude (m)
CV	Coefficient of variation
D_d	Droplet diameter ($\times 10^{-6}$m)
D_p	Diameter of micro-screen pore ($\times 10^{-6}$m)
$\overline{D}$	Sauter mean diameter of droplets ($\times 10^{-6}$m)
F_B	Buoyancy (N)
F_{Ca}	Capillary force (N)
F_D	Drug force (N)
F_{st}	Static force (N)
h	Distance from micro-screen surface to the top of droplet (m)
k_x	Wall correction factor
$V_{M,0}$	Maximum velocity of micro-screen in the harmonic oscillation (m/s)
V_M	Velocity of micro-screen at time t (m/s)
V_0	Maximum relative velocity of continuous phase (m/s)
V	Relative velocity of the continuous phase (m/s)
V_d	Relative velocity between droplet and continuous phase at $y = D_d/2$

Greek letters

γ	Interfacial tension (N/m)
δ_s	Stokes layer length (m)
μ	Viscosity of the continuous phase (Pa·s)
ν	Kinematic viscosity of the continuous phase (m^2/s)
ρ_c	Density of the continuous phase (kg/m^3)
ρ_d	Density of the dispersed phase (kg/m^3)
τ	Shear stress (Pa)
ω	Angular velocity (rad/s)

Chapter 1 Introduction

Emulsions are homogeneous mixtures of usually two immiscible phases with significant values in chemical, cosmetic, food and pharmaceutical industries. They are manufactured by dispersing one phase (the dispersed phase) into the other immiscible phase (the continuous phase) in the presence of surface-active agents (emulsifiers) to prevent emulsions from coalescence.

In conventional emulsification techniques, such as high speed stirring systems, rotor-stator systems and high pressure homogenizer systems, emulsions are produced by shearing two phases using a large amount of power input. The generated turbulent eddies break the dispersed phase up to small droplets (Walstra 1993). The problem is that, turbulent eddies are hard to control precisely in vessels, leading to difficulties in achieving the tunable size and narrow size distribution emulsions. Furthermore, the high power input could also create detrimental effects on thermal or stress sensitive ingredients in the case of food and pharmaceutical products.

Emulsions with good size controllability and uniformity are highly in demands in industry, as they can fulfill various intended uses and further functionalization. Membrane emulsification, one of alternative techniques, has been extensively investigated in recent years in order to realize this goal. In contrast to the droplet breakage mechanism, the droplet growth mechanism is adopted in the membrane emulsification. The dispersed phase is forced to go through the membrane pores and forms small droplets individually from each pore in contact with the continuous phase. In the early investigations, the cross-flow of continuous phase was used to generate shear stress to cut droplets off the membrane surface. Both experimental work and theoretical models have been done (Peng and Williams 1998; Gijsbertsen-Abrahamse, Van Der Padt et al. 2004; Hao, Gong et al. 2008). To intensify the relative motion between the two phases, the rotating membrane system has been developed (Vladisavljevic and Williams 2006; Aryanti, Hou et al. 2009). These studies all proved that the membrane

emulsification technique could produce emulsions with well-defined size and narrow size distribution. Moreover, the input of power was reduced dramatically. Hence, the process not only can produce emulsions in mild conditions, but also lower the energy cost (Pawlik and Norton 2012). It is reported that the cross-flow velocity, the rotating speed, the flux of dispersed phase, the type of surfactant, the surface wettability of membrane, collaboratively affect the quality of emulsions.

Although the membrane emulsification offers many advantages, there are still some drawbacks needed to be overcome. For the static membrane mode, the high-concentrated emulsions are hardly prepared, since a relatively high continuous phase volumetric flowrate should be applied. If the continuous phase is circulated through a pump, the pre-made emulsions could possibly be destroyed inside the pump, especially for fragile products. For the rotating membrane mode, the low porosity of membrane limits the emulsion throughput. In addition, the cost of membrane is another problem in the respect of commercial applications.

To further improve membrane emulsification techniques, we have designed a novel membrane emulsification apparatus with an oscillatory micro-screen module. In this system, the dispersed phase is pumped out from the micro-screen. The shear stress employed for initiating droplet detachment is generated by the micro-screen's "up and down" oscillatory motion. Two parameters, oscillation amplitude and oscillation frequency, can be regulated to control the shear stress more accurately and more range-widely, comparing with only one in the static and the rotating mode. Metal micro-screen with high porosity (36%) has been selected to fix on the system. It is generally agreed before that high porosity screens are not suitable for membrane emulsification because of coalescence of droplets between adjacent pores. However, no obvious droplet coalescence has been found on the oscillatory micro-screen in this system. Therefore, emulsion throughput has been largely improved with this high porosity micro-screen. Moreover, emulsion concentration is only dependent with time in the oscillatory system. As a result, emulsion products with high concentration can be achieved. All these improvements make the oscillatory micro-screen emulsification system more probably apply in industrial applications.

This thesis consists of 7 chapters and follows the "monograph" format as outlined by the Master's Programs of GENERAL THESIS REGULATIONS by the School of Graduate and Postdoctoral Studies (SGPS) in the University of Western Ontario. A summary of each chapter is listed below:

In Chapter 1, a general introduction is provided. The background, innovations and contributions of this project are stated, as well as the thesis structure.

In Chapter 2, a literature review shows the development history of the emulsification techniques. The membrane emulsification techniques are reviewed in details. Finally, the applications of membrane emulsification are illustrated.

In Chapter 3, the oscillatory micro-screen emulsification system is presented. The experimental materials, experimental procedures and characterization methods are provided.

In Chapter 4, the experimental results are discussed to illustrate the controlling factors on the droplet size and the size distribution, such as oscillation amplitude, oscillation frequency, oil phase flux, emulsifiers and shear stress.

In Chapter 5, the theory of micro-screen emulsification and the droplet formation mechanism are described. A force analysis has been carried out, which provides the basis for the modeling. Finally, the comparisons between the modeling results and the experimental results are shown.

In Chapter 6, the effects of the surface geometries of the continuous phase container's wall on the emulsion quality have been studied.

In Chapter 7, the conclusions and recommendations of this project are summarized.

Chapter 2 Literature review

2.1 Emulsion and emulsification

Emulsions are homogeneous mixtures of usually two immiscible phases, which are a class of colloids, a broad kind of materials with two phase dispersion. In especial, Emulsions generally represent the colloids which two phases are both liquid. They are manufactured by dispersing one phase (the dispersed phase) into the other immiscible phase (the continuous phase) in the presence of surface-active agents (surfactants). The process to prepare emulsions is called emulsification.

Dispersed phases are usually in the form of droplet in order to minimize the surface tension. Emulsifiers are substantially required in the emulsification process, because they are able to lower the interfacial tension of newly formed interface to ensure the kinetic stability of droplets. The good droplet stability is an important quality of emulsions, which means droplet size would keep unchanged during a long time. Emulsifiers can be classified to two types according to the solubility. Some emulsifiers are water soluble, such as Tween®, SDS, DTAB, etc. which have high values of hydrophilic–lipophilic balance (HLB). They are usually applied in oil-in-water emulsions. In contrary, some are oil soluble with low values of HLB, such as Span®, Brij®, PPG, etc. They are better for water-in-oil emulsions (Stang, Karbstein et al. 1994). The concentration of emulsifier should match the expected concentration of emulsion, since emulsifier molecules are continuously depleted as new droplets form. In addition, emulsifiers are sometimes used in both the continuous phase and the dispersed phase so that the spontaneous effect of two emulsifiers on the interface and the rapid adsorption dynamics are achieved.

Emulsions have significant values in the chemical, cosmetic, food, pharmaceutical industry and so on. Emulsions can be used in surface treatment because of the ability that can disperse oil substances into an aqueous phase homogeneously. This can avoid the use of toxic organic solvents. Food and cosmetic industries have demands for emulsions due to their rheological properties which may vary from a Newtonian liquid to an elastic

solid. Emulsions are also prepared for medical uses as carriers to tune the drug release rate or to control the target delivery. Here, multiple structured emulsions, which the dispersed phase droplets contain the continuous phase droplets, have been one of attractive and challengeable emulsification applications. To satisfy the product quality, several parameters of emulsions, such as droplet size, uniformity, stability, emulsion compositions, etc. had better be precisely controlled.

2.2 Emulsification techniques

2.2.1 Conventional techniques

Emulsification techniques have been developing for 40 years. In the industrial-scale production, the conventional emulsification techniques are widely used, such as the high-speed stirring homogenizer, the rotor-stator system and the high pressure homogenizer.

In the high speed stirring homogenizer, the dispersed phase is ruptured into fragments by the strong shear stress in vortices generated by a high-speed rotating paddle. However, the input energy density (a measure of input energy per unit volume) hardly distributes uniformly, even though it can be modified by the optimization of paddle geometry and configuration, as a result the droplet size distribution is bad. Therefore, this technique is usually used in the premixing step to prepare coarse products. As follows, coarse emulsions will be manufactured through other techniques to narrow the size distribution.

In the rotor-stator system, emulsions are formed in the limited space between rotor and stator. The shear stress is caused through the relative motion of rotor and stator. This technique is particularly effective for the emulsions in a viscous continuous phase. The narrow droplet size distribution would be obtained by precisely controlling the energy density (Schubert and Armbruster 1992).

In the high pressure homogenizer, the two phases or the premixing emulsions are pressed by high pressure into the mixing chamber through a nozzle. The dispersed phase is broken up under the effect of shear stress, cavitation and impact (Soon, Harbidge et al. 2001). The effects of emulsifier concentration, applied pressure and nozzle design on the

droplet size and uniformity have been studied by many researches. It is found that the formation of droplets is in a dynamic balance of breakup and coalescence, and the emulsifier concentration largely affects this process (Lobo, Svereika et al. 2002; Lobo and Svereika 2003). Large degree of coalescence occurs in the lower emulsifier concentration. The droplet size is related with the emulsifier concentrations but independent of the applied pressure. Droplet sizes varying from 50 to 350nm are obtained in the higher emulsifier concentration with less presence of coalescence, because the emulsifier is able to lower the interfacial tension and further facilitate the rupture of droplets. An advantage of this technique is high productivity, which is attractive in commercial applications.

Gijsbertsen-Abrahamse et al. (Gijsbertsen-Abrahamse, Van Der Padt et al. 2004) have made a statistics of the energy cost for different emulsification techniques, as shown in Figure 2.1.
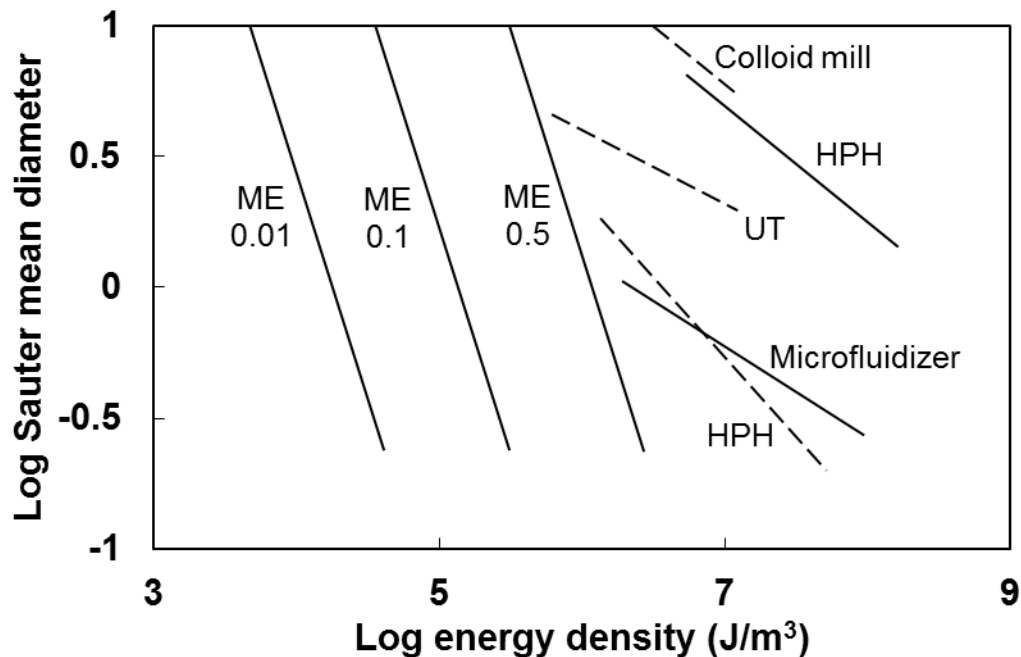
Figure 2.1   The average droplet size varies as a function of the input energy density for different emulsification techniques (Gijsbertsen-Abrahamse, Van Der Padt et al. 2004)

ME represents cross-flow membrane emulsification from (Nakashima, Shimizu et al. 1991) in which the numbers indicate the dispersed phase fraction. HPH is short for high pressure homogenizer. UT is short for Ultra Turrax. The solid line data is from (Schroder 1999).The dash line data is from (P. Walstra 1998). It is easily seen that the conventional emulsification techniques require a larger amount of energy, but only a part of it is used for the rupture of dispersed phase. Gijsbertsen-Abrahamse et al. (Gijsbertsen-Abrahamse, Van Der Padt et al. 2004) also pointed that 99.8% of input energy is lost and converts to heat in high pressure homogenizers. In the respect of economic issues, these conventional emulsification techniques are highly energy-consuming. On the other hand, the high energy density and the generated heat would be detrimental effects to the ingredients which are stress-sensitive or thermal-sensitive, especially in medical and food industries. In contrast, the membrane emulsification process is more efficient, and droplets form under the relatively mild conditions. Besides, in the membrane emulsification technique, the droplet size can be easily controlled and the narrow size distribution can be obtained. The details of membrane emulsification will be presented in next section.

2.2.2   Membrane emulsifications

Membrane emulsification techniques have been developed since 1990s and many processes have been designed. The principle of membrane emulsifications is the droplet formation mechanism, other than the dispersed phase breakage mechanism in the conventional techniques. The continuous phase and the dispersed phase are usually on the two side of membrane. The dispersed phase is pressed into the continuous phase through the membrane pores and forms droplets at the end of membrane pores. The shear stress caused by the continuous phase cuts droplets off (shown in Figure 2.2).
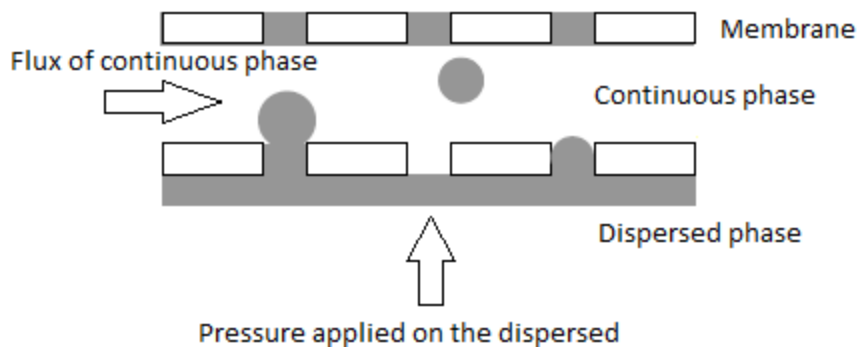
Figure 2.2   Schematic diagram of the mechanism of
membrane emulsification
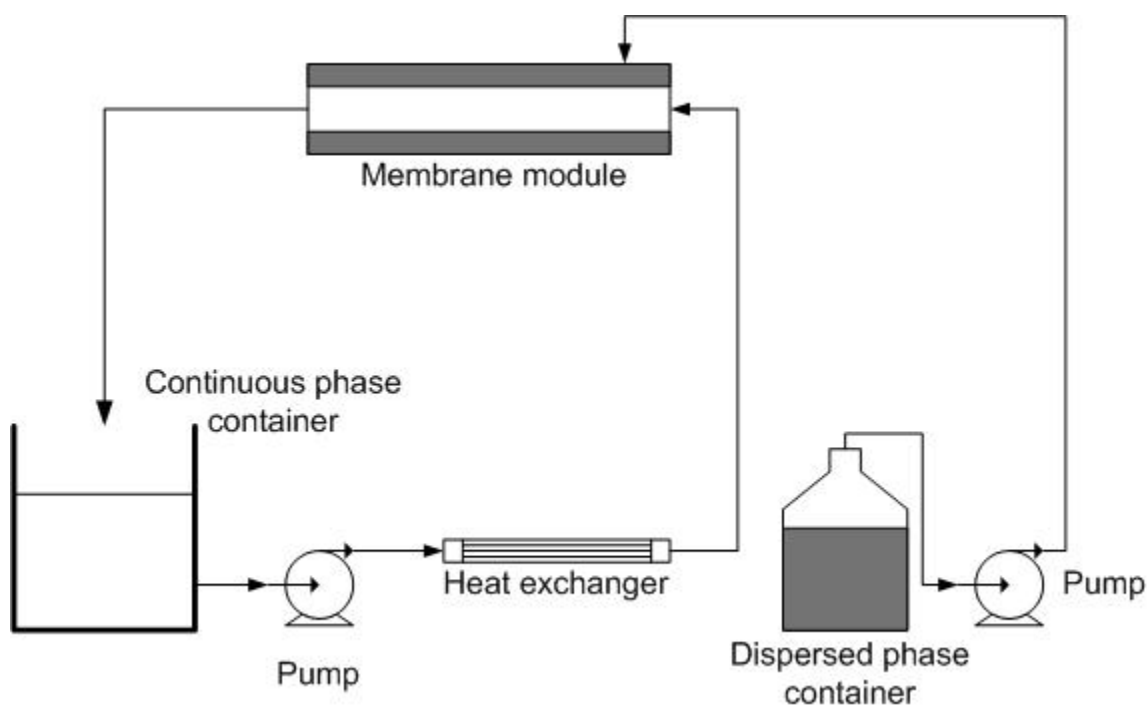
Figure 2.3   Schematic diagram of a general membrane
emulsification system

Figure 2.3 shows the basic system of membrane emulsification. The dispersed phase is forced into the membrane module by a compressed gas or a pump. The tubular membranes are usually used. The continuous phase is driven by a pump and it can be circulated for preparing the high concentrated emulsion.

On the basis of different ways to generate the shear stress, the cross-flow membrane emulsification and the rotating membrane emulsification have been investigated. According to the different operation processes, the one-trip, repeated emulsification and premixing process have been adopted. Various types of membrane of different materials, such as ceramic, polymer and metallic membrane, and of different parameters, such as pores size and porosity, have been used. Moreover, the effects of emulsifiers and the process conditions on the emulsion quality also have been well investigated.

The cross-flow membrane emulsification process is the most basic technique. The membrane unit keeps static. The continuous phase flows across the surface of membrane generating the shear stress to cause the detachment of droplets. The droplet size and size distribution are determined by three groups of parameters: 1) membrane properties, such as the membrane pore size, pore opening shape, porosity and surface wettability; 2) process conditions, such as the velocity of continuous phase, the flux of oil phase, etc.; 3) preparation conditions, such as the emulsifier type, emulsifier concentration and emulsion concentration.

According to the droplet formation mechanism, the average droplet size is largely determined by the membrane pore size (Mine, Shimizu et al. 1996; Peng and Williams 1998). Many experimental data show that there is a linear relationship between the average droplet size and the membrane pore size (Peng and Williams 1998):

$$D_d = kD_p$$

(2.1)

where D_d and D_p are denoted as the droplet size and pore size respectively. The value of k ranges from 2 to 8 in the cross-flow emulsification process depending on the proper preparation conditions. If the requirement is not fulfilled, the value of k will be much larger than that shown above due to severe coalescence. For the cases which the pore

opening shapes are not circular, the equivalent pore diameter should be used. Additionally, the uniform membrane pore size is also expected to manufacture "monodispersed" emulsions.

Kobayashi et al. (Kobayashi, Nakajima et al. 2002) found that the shape of membrane pore opening did affect the average droplet size using the silicon membrane with elongated holes under a low continuous phase velocity. The average size of droplets prepared through the non-circular pores was smaller than that of droplets prepared using the same material membrane but with the circular pores of the equivalent diameter. The equivalent diameter is defined as the diameter of a circle with the same area of the non-circular shape. Besides, the size of droplets from elongated pores was independent with the cross-flow velocity and transmembrane pressure drop, while that was not for droplets from circular pores.

The high porosity of membrane can facilitate a large throughput of emulsions in the respect of commercial applications. However, the high porosity has a negative effect for the droplet size distribution, as droplets could touch each other and further coalesce at adjacent pores. Computational fluid dynamics calculations suggested that the membrane porosity should better be as small as 1.5% in order to prevent droplets recombination (Abrahamse, Van der Padt et al. 2001). Abrahamse et al. have analyzed the droplet formation process using a high speed camera (Abrahamse, Van Lierop et al. 2002). It was concluded that the distance between pores should be larger than the average droplet size, because such distance should be left for the droplets deformation in the direction of the continuous flow. Despite the fact that high porosity would probably cause coalescence, membranes with high porosity still have been studied in many experiments (Vladisavljevic and Schubert 2002; Wagdare, Marcelis et al. 2010). The porosity of SPG membrane is in the range of 53-60% and that of micro-engineered micro-screen can reach to 30%. In fact, only a small part of membrane pores was active in the process (Vladisavljevic and Schubert 2002). The fraction of active pores increases with the increase of transmembrane pressure. As a result, the dispersed phase flux increases as well.

The membrane wettability affects the droplets uniformity as well. The membrane surface should not be wetted by the dispersed phase (Joscelyne and Tragardh 2000). The O/W emulsions with wide size distribution would be produced if the membrane surface is hydrophobic, which was proven by Nakashima et al. (Nakashima, Shimizu et al. 1991). Therefore, the hydrophilic surface membrane is suitable for O/W emulsions and the hydrophobic surface membrane is applicable in the W/O emulsions preparation.

The relative motion between the continuous phase and the membrane generates the shear force which is the major detachment force exerted on droplets. The higher velocity of continuous fluid the stronger shear force (shear stress) is created. Evidently, the average droplet size decreases as the cross-flow velocity increases, and the decreasing rate becomes smaller and smaller till closes to zero at a stable value (V. Schröder 1997; V. Schröder 1997), as shown in Figure 2.4. Therefore, the cross-flow velocity can be used to adjust the droplet size, and it is convenient to control. However, when the droplet size gets close to the boundary layer or into it, the droplet size becomes independent of the cross-flow velocity. On the other hand, if the droplet size decreases closing to the diameter of membrane pores, the pore size will be a limitation as well.
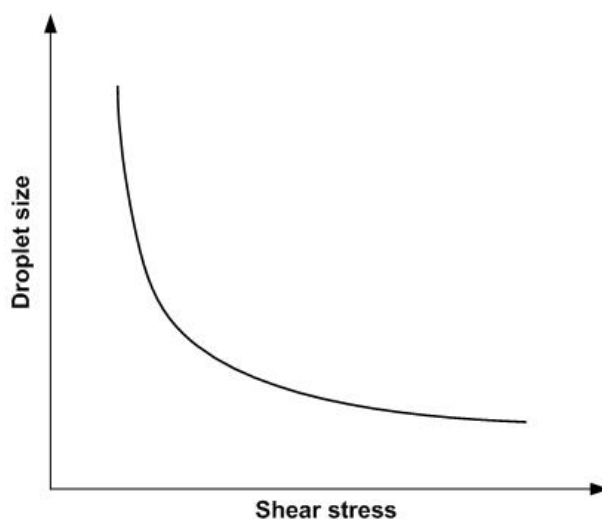
Figure 2.4   Schematic plot of the relationship between the shear stress and the droplet size (V. Schröder 1997)

The membrane emulsification process can be divided into two stages theoretically, the growth stage and the detachment stage (Peng and Williams 1998). In the growth stage, the newly formed droplets increase in size. When the droplet size becomes large enough such that the drag force caused by shear stress starts to push it away from the membrane surface, the detachment stage starts. In fact, the detachment of droplet takes some time, as a result the droplet size is larger than that at the end of growth stage. Therefore, the dynamic growth in the detachment process should be taken in consideration (Hao, Gong et al. 2008). Thus, the dispersed phase flux has effects on the droplet size, especially in the low shear stress region. The droplet size increases as the dispersed phase flux increases. Besides, the emulsion productivity increases as well with the increase in the dispersed phase flux. However, Schröder et al. have studied the effects of emulsifier adsorption dynamics in the droplet formation process (Schroder, Behrend et al. 1998). If the surfactant adsorption dynamics is such rapid that the interfacial tension decreasing time is shorter than the detachment time, the interfacial tension dynamics have a little or no influence on the droplet size and the size remains unchanged upon the increasing flux.

Emulsifiers play two roles in emulsification process. Firstly, they are able to lower the interfacial tension between two immiscible phases. The more effective emulsifiers the more interfacial tension can be reduced. The low interfacial tension can facilitate the breakup of dispersed phase. Meanwhile, emulsifiers act as the stabilizer to prevent droplets coalescence. This is decided by the type of emulsifier and the emulsifier concentration. As reported by Peng and Williams (Peng and Williams 1998), the capillary force caused by the interfacial tension is the main force to keep droplets attaching on the membrane surface. Therefore, if the interfacial tension decreases, the droplet size becomes smaller. The interfacial tension between the continuous phase and the dispersed phase performs as a function of time, although the time is very short around 1s. Hence the emulsifier molecule adsorption dynamics should be considered. It is proven experimentally by Schröder et al. that the size of droplets prepared in SDS solution was smaller than that of droplets in Tween20 solution, because SDS moves and adsorbs faster than Tween20 (Schroder, Behrend et al. 1998). Vladisavljevic et al. (Vladisavljevic, Surh et al. 2006) have studied the influences of various emulsifiers on the average droplet size and the transmembrane flux using the shirasu porous glass (SPG) membrane with the

mean pore size of 5µm. The maximum flux of the dispersed phase in the Tween 20 solution (5-47 $m^3/m^2 \cdot h$) was smaller than that in the SDS solution (29-60 $m^3/m^2 \cdot h$), because less energy was required for the breakage of a SDS stabilized droplet due to the lower interfacial tension. The mean particle size stabilized by SDS is smaller as well. In order to prepare the monodipersed emulsions and improve the emulsion throughput, the bi-emulsifier system which uses emulsifiers in both phases is applied in the membrane emulsification process. Wagdare et al. (Wagdare, Marcelis et al. 2010) have compared the effects of a variety of emulsifiers in a single phase and in the double phases using a silicon micro-engineered micro-screen with high porosity. It was shown that the Span80/SDS and the Span80/Tween20 system promoted good droplet formation particularly under the high dispersed phase flux. The newly formed interfaces were covered by emulsifier molecules faster in the case that two types of emulsifiers were affecting on the both sides of interface spontaneously.

Spyropoulos et al. (Fotios Spyropoulosa 2011) have investigated the influences of emulsifier concentration using SPG membrane with 1µm pores to prepare 1% sunflower oil O/W emulsions. It is reported that the average droplet size was inversely proportional to the emulsifier concentration. Between the concentration of 0.01% and 0.4%wt, the average droplet size decreased rapidly with the surfactant concentration increasing. And the higher HLB (hydrophilic-lipophilic balance) of the emulsifier, the faster the droplet size decreases. SDS, Tween20 and Tween80 have the same effect on the droplet size. This phenomenon can be explained by the emulsifier adsorption dynamics as well.

The rotating membrane emulsfication is a relatively novel technique and it has been developed since approximately 10 years. The droplet detachment is initiated by the rotating motion of membrane in comparison of the cross-flowing continuous phase. The tubular stainless steel membranes with uniform pores penetrated by laser have been widely used so far. In this system, the dispersed phase is pressed to the center of tubular porous membrane and goes through pores in the radial direction. This technique can manufacture emulsions of a wide range of concentration without circulating the continuous phase as the cross-flow membrane emulsfication does, which avoids the

disruption of droplets during going through the pump. Therefore, the rotating membrane emulsification is more practical in commercial applications.

The rotating membrane emulsification has the same mechanism of emulsion formation as the cross-flow membrane emulsification described above. And the controlling factors, such as the membrane pore size, porosity, emulsifier type, emulsifier concentration, and the dispersed phase flux, etc., keep the similar influences on the droplet size and the emulsion uniformity, but a new parameter--the membrane rotating speed. A rotating membrane emulsification system was designed by Vladisavljevic et al. using a stainless steel membrane with 100μm laser drilled pores to prepare O/W emulsions with 2wt% Tween20 as the emulsifier (Vladisavljevic and Williams 2006). The emulsions with the average size of 104-107μm and the very narrow size distribution (coefficient of variation (CV) <20%) were prepared. It is noted that the droplet size is smaller than two times of the pore diameter. This work also showed that the droplet size decreased as the emulsifier concentration, membrane rotating speed and continuous phase viscosity increased. These results obey the manners obtained from the cross-flow membrane emulsification. It is evidenced by Aryanti et al (Aryanti, Hou et al. 2009) using the tubular stainless steel membrane with the mean pore size of 100μm and the porosity of 3% to prepare the paraffin wax-in-water emulsions with Tween20 or SDS as the emulsifier and carbomer as the stabiliser. The average droplet size ranged from 80 to 570μm with the CV between 10%-30%. The membranes with different shape (square and rectangular) slotted pores were used in the rotating membrane emulsification by Yuan et al (Yuan, Aryanti et al. 2009). It is found that the square and rectangular pores were beneficial for the emulsions uniformity, which the CVs (~10%) of emulsions were both smaller than that of emulsion prepared from circular pores. The droplet size was also determined by the dispersed phase flux, membrane rotating speed and the equivalent pore diameter. The droplet formation rate was affected by the orientation of pores, which could be optimized for a higher emulsion throughput.

Another approach to decouple the continuous phase flow from the shear is oscillatory motion. This would also provide the necessary shear for droplet detachments that is independent of the crossflow, and eliminates the need for flow circulation. Two

parameters, oscillation amplitude and oscillation frequency, can be regulated to control the shear stress more accurately and more range-widely, comparing with only one in the static and the rotating mode. Furthermore, the input energy density in an oscillatory system can be lower than that in other dynamic membrane systems (Gomaa, Rao, Al-Taweel 2011).

The oscillatory membranes have very few applications in emulsification. Holdich et al. have compared the emulsions prepared using a tubular needle oscillating membrane and a rotating disc over stationary membrane (Holdich, Dragosavac et al. 2010). It is found that the oscillatory system gave smaller and more uniform drops. This agreed with the simulations of the effect of vibration on a single droplet formation (Kelder, Jansen et al. 2007). The combination of oscillation and crossflow membrane emulsification has been investigated (Holdich, Dragosavac et al. 2013). It is found that droplet size can be reduced and better controlled.

Other membrane emulsification processes also using the droplet formation mechanism have been designed, such as the stirred cell membrane emulsification (Kosvintsev, Gasparini et al. 2005; Stillwell, Holdich et al. 2007; Dragosavac, Sovilj et al. 2008; Egidi, Gasparini et al. 2008; Dragosavac, Holdich et al. 2012). The dispersed phase is forced to the continuous phase by penetrating a static flat membrane. The "push-off" shear force is caused by the vortices driven by a stirred paddle above or below the membrane. The emulsions with a very low CV (~10%) can be prepared. The membrane properties, process conditions and preparation conditions have the similar effects on the droplet size and the size distribution as described above.

In addition of the membrane emulsification process, other new techniques have been developed to prepare monodispersed emulsions, for instance microchannels (Sugiura, Nakajima et al. 2000; Kobayashi, Nakajima et al. 2003), microcapillaries (Utada, Lorenceau et al. 2005), and microfluidic devices (Abraham, Eun Ho et al. 2006; Garstecki, Fuerstman et al. 2006; Song, Chen et al. 2006; Seo, Paquet et al. 2007; Lingling, van den Berg et al. 2009). Although much more uniform emulsions can be

prepared, the low productivity hinders these techniques' applications in industry. The scale-up problem is needed to be solved in the future.

2.3   Applications of membrane emulsification

Emulsions have been widely applied in the food, pharmaceutical, cosmetic and coating industry. Except making the basic liquid-liquid emulsions, membrane emulsification techniques have been expanded to synthesize microparticles at the ease of advantages of the controllable particle size and the narrow size distribution. Emulsions are usually in the liquid phase, but it is possible to transfer the liquid to the solid or partially solid phase by controlling temperature (Weiss, Decker et al. 2008). In these cases, the membrane emulsification process should be carried out above the temperature of the material melting point. After the formation of emulsions, the prepared droplets will be solidified or crystalized by cooling the temperature below the melting point. Solid lipid nanoparticles can be synthesized by this process, which the oil phase has been fully or partly solidified (Muller, Radtke et al. 2002). Emulsions can be transformed to particulates through polymerization or gelation as well (Vladisavljevic and Williams 2005). For instance, the organic phase droplets containing monomers are possibly transformed to the solid polymer by heat-induced polymerization or interfacial polymerization with introducing initiators (Yuan, Williams et al. 2010). Multi-structured particles, such as the particles embedded with another solid particles or liquid droplets (Nakashima 2002), the foamed particles, the hollow particles (Gao, Su et al. 2009) etc., are able to be prepared by using the multiple emulsions as templates.

Nevertheless, the current commercial products are almost the conventional emulsions, such as the oil-in-water and water-in-oil system. Nowadays, emulsion products can be functionalized by novel structures, for example encapsulation, multilayers, colloidosomes, microclusters, etc. (McClements 2012). The membrane emulsification techniques have several advantages in the preparation of multiple emulsions than the conventional techniques.

The multiple emulsions are defined as the smaller continuous phase droplets embedding in the dispersed phase droplets forming the O/W/O or W/O/W emulsion system, and are also called duplex or double emulsions. In medical engineering, the multiple emulsions can be used as the carriers in the drug delivery (Couvreur, Blanco-Prieto et al. 1997; Vladisavljevic, Shimizu et al. 2006) and the supporters in the drug release (Olivieri, Seiller et al. 2003; Dragana Vasiljevic 2006). In the food industry (Lesmes and McClements 2009), the multiple emulsions can be used to lower the fat content by filling up the internal volume of oil droplets with aqueous solution. Besides, they also can be used to reduce the density difference between the emulsion droplets and the continuous phase in order to prevent emulsion creaming.

The multiple emulsions are typically manufactured by two steps (Pawlik and Norton 2012). For example, in $W_1/O/W_2$ system, firstly, the coarse emulsions are prepared by shearing the water phase 1 into the oil phase in the conventional emulsification apparatuses, such as the high-speed stirring, high pressure homogenizer and rotor-stator system. The second step is to disperse the prepared coarse emulsions into the water phase 2. The membrane emulsification should be the best candidate for the second step. It performs efficiently with the low energy density, which the multiple emulsions can form under mild conditions. The breakage of the multiple structures can be minimized. On the other hand, the external droplet size can be controlled precisely for an expected encapsulation ratio.

Many investigations have been done to study the effects of membrane emulsification conditions on the droplet size, size distribution, encapsulation and tracer release rate in the multiple emulsion system (van der Graaf, Schroen et al. 2005). The encapsulations of W/O/W emulsions prepared by the membrane emulsification process and the stirring process have been compared by Okochi et al (Okochi, Nakano 1997). It is found that the encapsulation of multiple emulsions produced by the membrane emulsification is higher than that from the stirring process due to the monodispersed external droplets prepared without very small ones. Jiao et al. have investigated the multiple emulsion stability associated with the inner and outer phase pressure and the interfacial film strength (Jiao, Rhodes et al. 2002). The multiple emulsion stability is determined by the interfacial film

strength of the hydrophobic surfactant layer between the oil phase and external water phase. And the stability of the multiple emulsions is also related to the osmotic pressure of the internal droplets and the Laplace curvature pressure. Pawlik and Norton have compared the encapsulation stability of the multiple emulsions prepared by SPG cross-flow membrane, SPG rotating membrane and rotor-stator techniques (Pawlik and Norton 2012). The duplex emulsion droplet size and encapsulation stability are both modified by the emulsification conditions inherent for each technique, which the cross-flow velocity and transmembrane pressure are for the crossflow process, the rotating velocity and transmembrane pressure are for the rotating membrane process, and the mixing time is for the high-shear mixer. The encapsulation stability was noted by the salt release which was the marker in the internal water phase. It is reported that the salt release rate of the emulsions prepared by the rotating membrane process is the lowest because of the smallest droplet size achieved. The larger droplet size, the more surface area is provided for the ionic diffusion. Moreover, the encapsulation stability is associated with the effecting time of shear force. It is proposed that the long existing time of shear force applied on droplets would jeopardize the homogenous coverage of emulsifier molecules by leaving a weak area. This reduces the strength of interfacial film. Jager-Lezer et al. have investigated the release kinetics of a water-soluble drug in the W/O/W multiple emulsion with different surfactant concentrations (Jager-Lezer, Terrisse et al. 1997). It is denoted that the drug release is controlled by the swelling mechanism of oil phase. The drug release rate is mainly decided by and reversely proportional to the lipophilic surfactant concentration. It is also speculated that the stability could be improved by increasing the lipophilic surfactant concentration, which could strengthen the interfacial film. In contrary, an excess of hydrophilic surfactant destabilizes the emulsion.

2.4　Summary and outlook

The conventional emulsification techniques, such as the high-speed stirring homogenizers, high-pressure homogenizers, and rotor-stator systems, have been widely applied to prepare emulsions in large-scale. However, it is not likely to control the droplet

size distribution within a narrow width due to the droplet breakage mechanism and the unpredictable hydrodynamics.

The development of membrane emulsification techniques has improved the quality of emulsion products in the tunable droplet size ranging from 0.5 to 100μm and the narrow droplet size distribution denoted by the coefficient of variation of 10%-30%. The droplet size and size distribution have been proven to be determined by the membrane properties, process conditions and preparation conditions. Typically, three membrane emulsification processes--the cross-flowing continuous phase process, the rotating membrane process and the stirred cell process, have been designed according to the ways to generate shear force.

Solid particles with high uniformity also can be manufactured by membrane emulsification processes in the presence of polymerization, crystallization, and gelation. The functionalized emulsions and particles associated with multiple structures which is a novel and attractive application of membrane emulsification have been realized as well. This type of products has a future potential as a carrier or supporter in the issues of drug delivery and drug release.

Membrane emulsifications have several advantages in the scale-up design, such as the repeatable manufacturing process, the independent unit operation and the continuous producing mode. However, they still haven't been utilized in the commercial production so far due to the low emulsion throughput. The scale-up design by multiplication of membrane modules is not desirable because of the increase of equipment cost and maintenance cost. Therefore, new membrane emulsification processes with high emulsion throughput are needed to be developed in the future.

Chapter 3 Experimental

This study consists of four major parts of work:

1. The oscillatory micro-screen emulsification system design;
2. The emulsion preparation under different process conditions in the Span80 (in oil phase)/SDS (in water phase) emulsifier system;
3. The emulsion preparation under different process conditions in the Span80 (in oil phase)/Tween20 (in water phase) emulsifier system;
4. The emulsion preparation in the container with different surface geometries of the wall facing micro-screen.

3.1 Apparatus

Two pieces of micro-screen are fixed on the both sides of the oscillatory module (shown in Figure 3.1). A peristaltic pump (Phamacia Fine Chemicals, P-3) pushes the oil phase into the oscillatory module via tubing, internal channel and further into the water phase through the micro-screen. The module's oscillatory motion is driven by a variable speed motor. The oscillation amplitude can be changed through an eccentric system which transfers the motor's circular motion to the micro-screen module oscillatory motion. The schematic illustration of the experimental setup is shown in Figure 3.2.
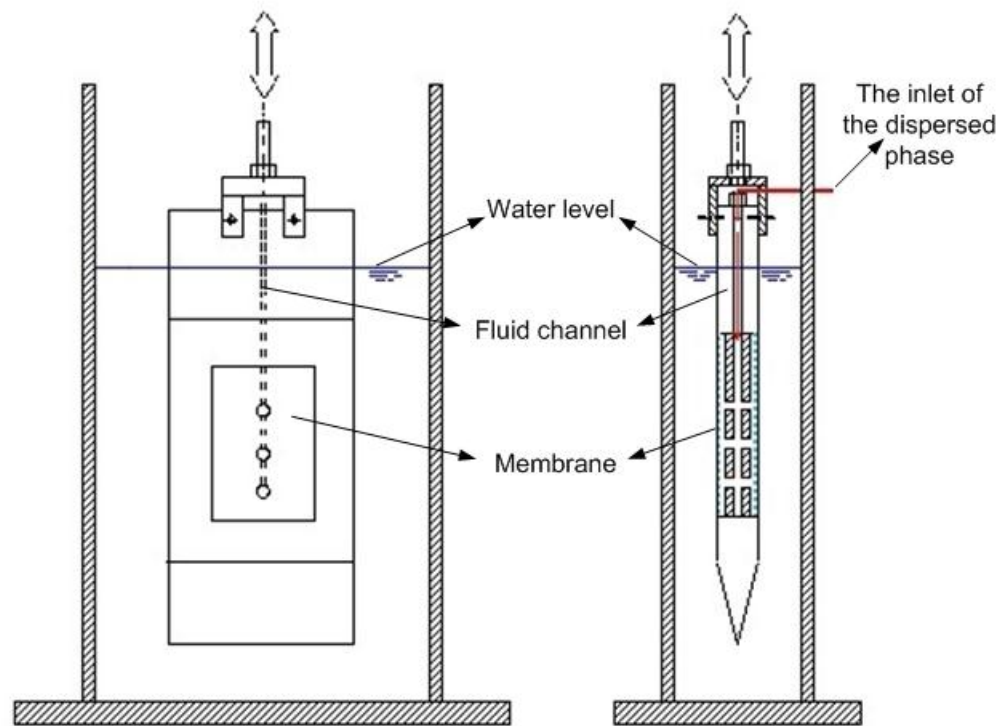
Figure 3.1   Schematic diagram of the oscillatory micro-screen module
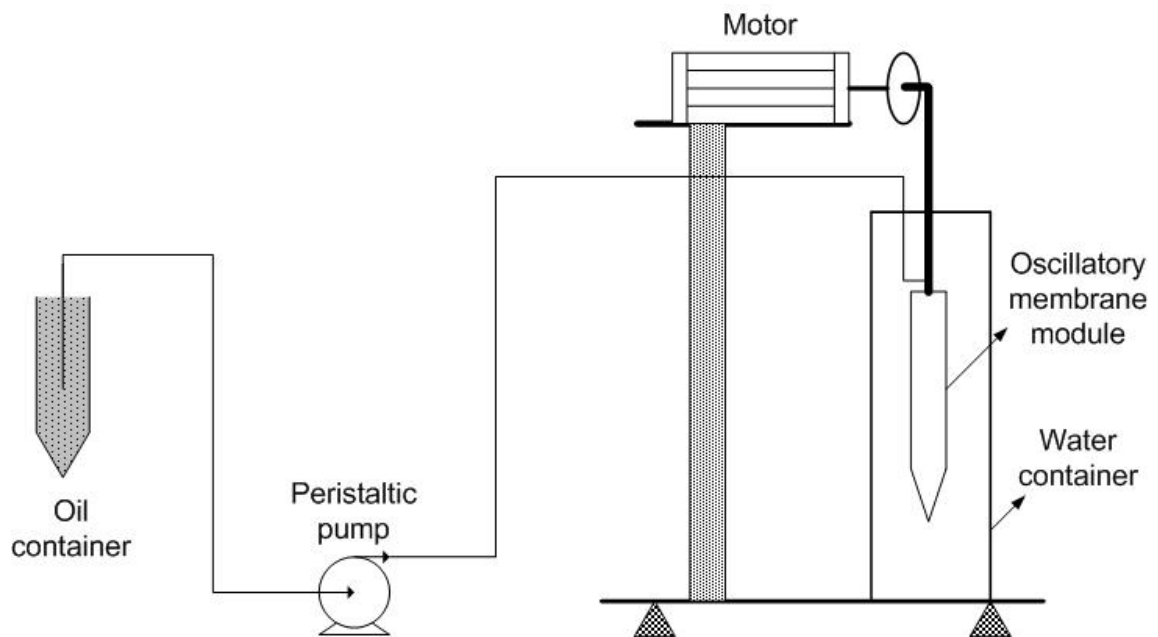
Figure 3.2   Schematic diagram of the system setup

3.2 Membrane selection

As a rule, the dispersed phase should not wet the membrane pores. This means that hydrophilic membranes are suitable for making O/W emulsions and hydrophobic membranes for W/O emulsions (Joscelyne and Tragardh 2000). Moreover, the high porosity is a potential positive feature, since to make the membrane emulsification process commercially attractive, sufficient porosity is necessary to ensure high productivity (Wagdare, Marcelis et al. 2010).

In the previous investigations, either membranes or micro-engineered sieves were studied, which in some cases suffered from low porosity, brittleness, and/or high cost. In this work, the corrosion-resistant stainless steel wire woven micro-screen (shown in Figure 3.3) purchased from McMaster-Carr was chosen. The micro-screen has the opening size of 0.0012'' (30.5µm) as rectangular shape, with the wire diameter of 0.0008'' (20.3µm), yielding a porosity of 36%. The equivalent diameter of rectangular pores is 34.39µm. The surface of the micro-screen is hydrophilic resulting from the property of stainless steel. Two pieces of micro-screen are fixed on the both sides of the oscillatory module. In the respect of commercial applications, the micro-screen possesses advantages of flexibility, durability, inexpensive, and the large porosity which offers it potential to reach high productivity.
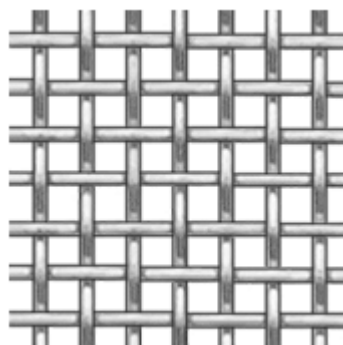
Figure 3.3   Schematic diagram of the stainless steel wire woven micro-screen

3.3   Materials

Common surfactants were chosen as emulsifiers both in water phase and oil phase. Sodium dodecyl sulphate 20% solution (SDS, $CH_3(CH_2)_{11}OSO_3Na$, Amresco) and Polyoxyethylene sorbitan monolaureate (Tween®20, $C_{58}H_{114}O_{26}$, Amresco) were dissolved respectively as the surfactant in distilled water which was the continuous phase. The concentration of SDS and Tween®20 was 1%w/v and 4%w/v respectively in order to keep close interfacial tensions. Sorbitane monooleate (Span®80, $C_{24}H_{44}O_6$, Sigma) was dissolved as a co-surfactant in the corn oil (purchased from supermarket, Mazola Company) which was the dispersed phase. The concentration of Span®80 was 1%w/v.

3.4   Experimental procedure

The micro-screen is required to be cleaned before every experiment. Firstly, distilled water was used to flush the micro-screen extensively. Then, the micro-screen was rinsed with ethanol and acetone. Finally, the micro-screen was washed thoroughly by distilled water again and dried at room temperature.

The oil phase with 1%w/v Span80 was filled in a graduated cylinder and the water phase with 1%w/v SDS or 4%w/v Tween20 was filled in the water container. After the fixation of modules and the connection of tubing, the air in the liquid pathway should be removed. A syringe was used to remove the air out via a three-way connection tubing.

In the emulsion preparation using the Span80/SDS and Span80/tween20 surfactant systems, 30mL of oil phase was pumped into 1000mL of water phase, and this composition was kept constant for all experiments under different conditions. Three oscillation amplitudes of 2mm, 6mm, and 10mm were selected to study. Under each amplitude, the apparent micro-screen flux of $8.3\times10^{-6}m^3/(m^2\cdot s)$, $13.8\times10^{-6}m^3/(m^2\cdot s)$ and $19.4\times10^{-6}m^3/(m^2\cdot s)$ was studied. The apparent micro-screen flux is defined as the dispersed phase volumetric flowrate over the area of micro-screen. Within each oil phase flux, the oscillation frequency was regulated in a wide range from 4.2Hz to 25.1Hz. One batch of emulsions was prepared under each set of process conditions. After finishing

each batch of emulsions, the water container and the micro-screen should be cleaned thoroughly for next experiment.

In the study of the effects of continuous phase container channel geometries, three types of surfaces have been investigated, which are the flat surface, the wavy surface and the surface with baffles, as shown in Figures 3.4, 3.5 and 3.6. These geometries were made on the foamed plastics inserts, because they are easy to manufacture. On the other hand, the inserts can reduce the container width in order to magnify the influence of surface geometry. The original width between the container wall and the micro-screen is 30mm. After inserting, the width reduces to 2mm.

In this series of experiments, the same operation procedure should be obeyed. All experiments were carried out in the Span80/SDS system using the oil phase flux of $13.8\times10^{-6}\text{m}^3/(\text{m}^2\cdot\text{s})$ to prepare 3% (O/W) emulsions. In the test of each type of insert, several oscillation frequencies were applied under the amplitude of 2mm, 6mm and 10mm.
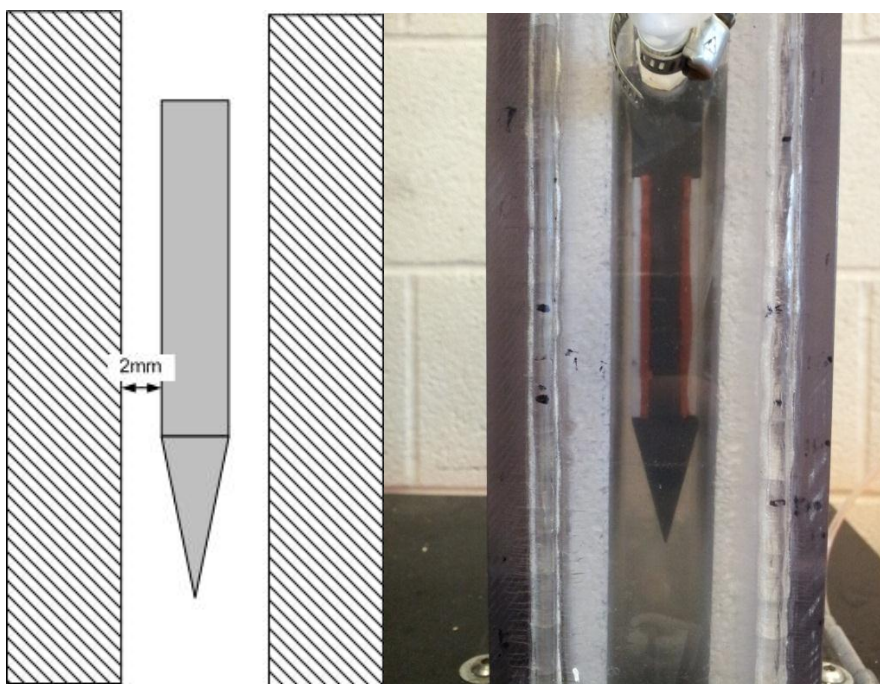
Figure 3.4   Schematic diagram and photo of the inserts with flat surface
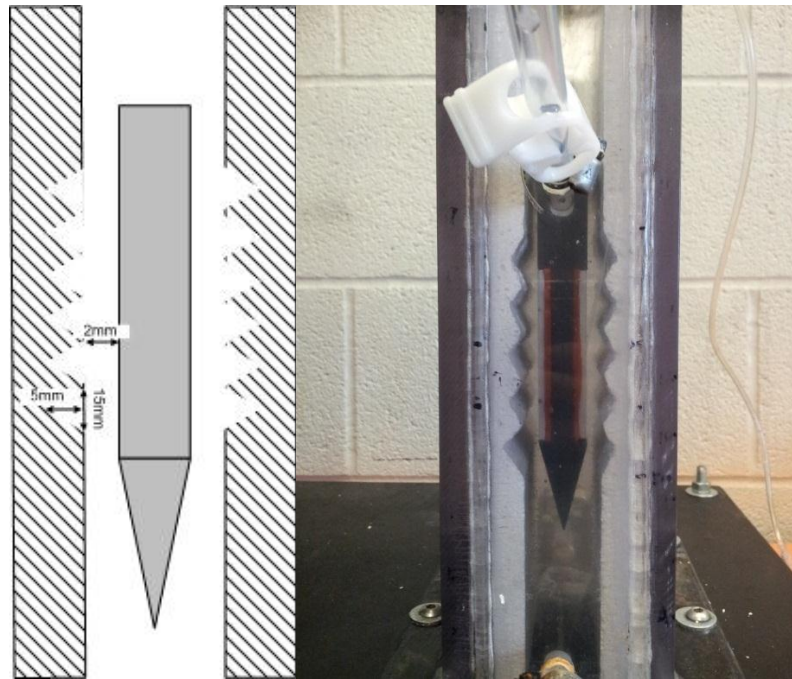
Figure 3.5   Schematic diagram and photo of the inserts with wavy surface
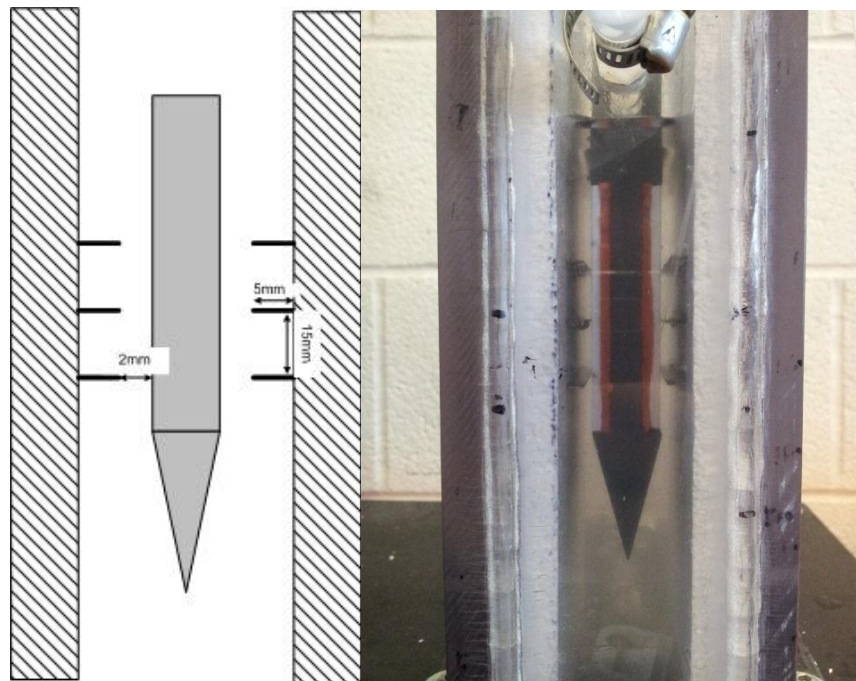
Figure 3.6   Schematic diagram and photo of the inserts with baffles

3.5 Emulsion characterization

Before taking samples, the prepared emulsions should be mixed mildly using a stirring stick to ensure the homogenization of product. Then, samples were taken from the middle part of the water container.

The pictures of prepared emulsions were taken by optical microscope (Omax microscope, M8311-PHB1-C50). Emulsion samples were gently stirred before analysis to ensure that they were homogeneous. A drop of emulsion sample was then placed onto a microscope slide. ImageJ software was used to analyze the captured pictures to obtain the emulsion droplet size. The images with scattered droplets (no aggregation) should be chosen for analyzing in order to ensure accuracy of measurement. Also these images should be taken randomly from different spots in samples. The droplet size distribution was calculated from at least 200 droplet diameters. Manual verification of the droplet size was also performed.

Sauter mean diameter is adopted to evaluate the droplet size as it is an average of particle size useful in fluid dynamics:

$$\overline{D} = \frac{1}{\sum_i \frac{f_i}{D_i}}$$

(3.1)

D_i is the individual droplet diameter,

and f_i is the volume fraction of this individual droplet.

The size distribution is expressed by the coefficient of variation (*CV*):

$$CV = \frac{\left[\sum_{i=1}^{n} \frac{(D_i - \overline{D})^2}{n} \right]^{1/2}}{\overline{D}}$$

(3.2)

The lower value of CV, more uniform droplet distribution is. CV of 40% was used as a criterion to determine whether emulsion product is uniform or not.

The interfacial tension at the oil/water interface was measured by the pendant drop method in the FTA1000 drop shape instrument (B Frame System, First Ten Angstroms). The result was analyzed by FTA video drop shape software. It is reported that the interfacial tension would decrease with time till to an equilibrium state (Schroder, Behrend et al. 1998). Here, however, the dynamic interfacial tension would come to equilibrium within a very short time on the effect of surfactants both in two phases. Therefore, the measured equilibrium interfacial tension could be used as the dynamic interfacial tension.

Chapter 4 Controlling factors on emulsion quality

4.1 Effects of process parameters
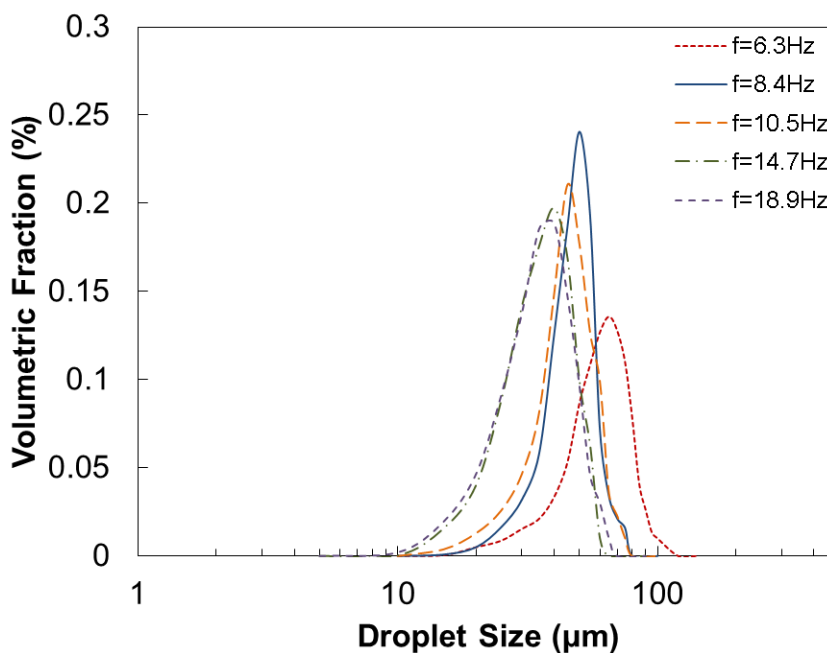
Figure 4.1 Droplet size distribution profile obtained in Span80/Tween20 system under oil phase flux=13.8×10^{-6}m^3/(m^2·s) and amplitude=6mm

Figure 4.1 presents the droplet size distribution profile obtained in Span80/Tween20 system under the oil flux of 13.8×10-6m^3/(m^2·s) and amplitude of 6mm. It is shown that the droplet size decreases with the increase of frequency. At the start frequency of 6.3Hz, the size distribution is wide. From 6.3Hz to 8.4Hz, the size distributions become narrow. But then, they become wider progressively again. There is an optimal frequency appearing around 8.4Hz in regard of droplet uniformity.

Figure 4.2 and Figure 4.3 show the variations of droplet size and size distribution as a function of oscillation frequency using the different oil phase flux of 8.3×10^{-6} m^3/(m$^2 \cdot$s), 13.8×10^{-6}m^3/(m$^2 \cdot$s) and 19.4×10^{-6}m^3/(m$^2 \cdot$s) at the amplitude of 6mm in the Span80(4%w/v)/SDS(1%w/v) bi-emulsifier system. Due to the presence of a large number of pores in the micro-screen, the number of active pores during the emulsification process is hard to determine. Hence, the oil phase flux is represented by apparent micro-screen flux, which is the oil phase volumetric flowrate per unit area of micro-screen. Figure 4.2 shows the effect of oscillation frequency on the average droplet size which varies from 70μm to 30μm. It is observed that in all cases the droplet size decreases with the increasing of oscillation frequency. The trend coincides with that in the distribution profile (Figure 4.1). This can be explained by the increase in shear stress, the major force driving the droplet detachment. With the oscillation frequency becoming larger, the shear stress increases leading to the droplet detachment off the micro-screen at smaller size. The decreasing rate of droplet size becomes slower at the high frequency regime, because the droplet size is close to the micro-screen pore diameter. It also can be seen that the droplet size does not obviously grow larger with the increase in oil phase flux. From the aspect of membrane emulsification mechanism, the dispersed phase flux does influence the droplet size in the detachment stage (Peng and Williams 1998). However, the high shear stress generated by the oscillatory motion makes the detachment process so short that the oil phase flux is unable to affect the droplet size statistically.
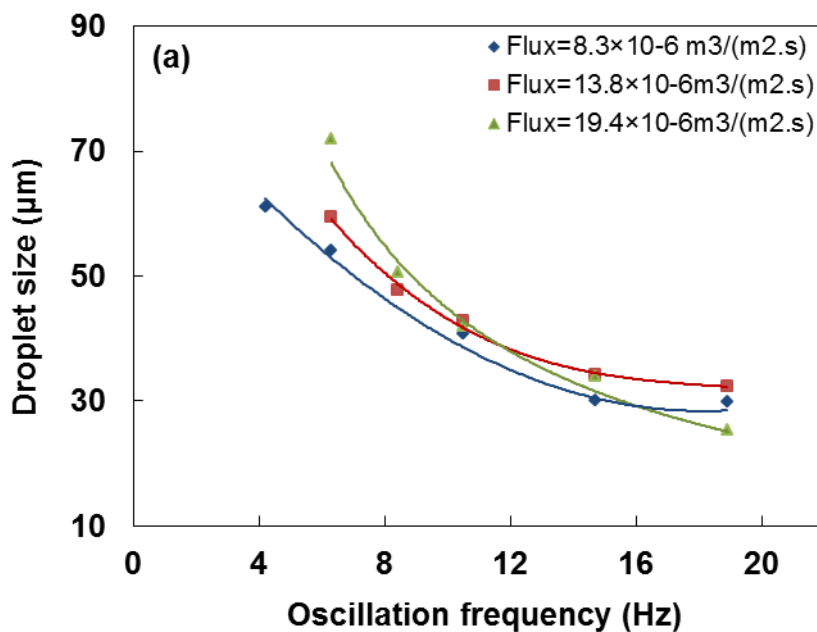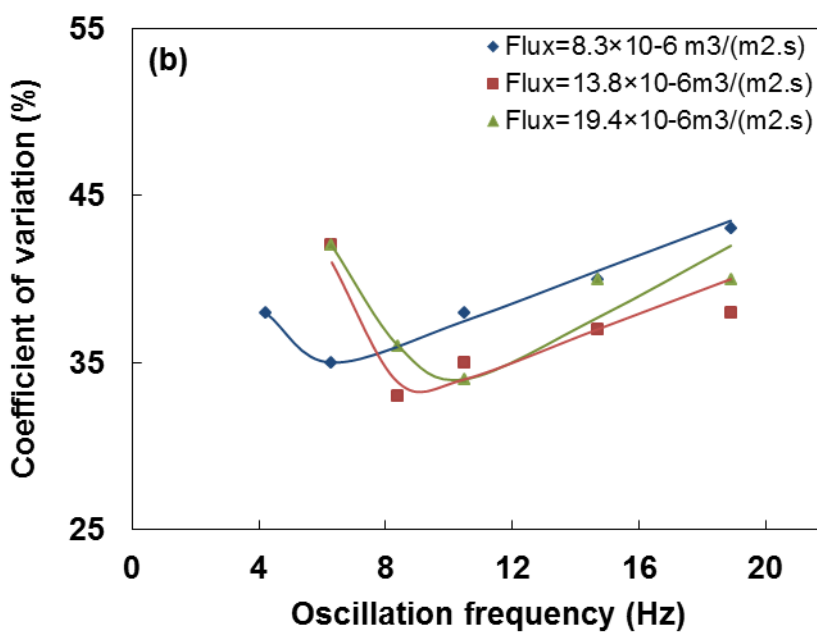
Figure 4.2

Figure 4.3

Effects of the oil phase flux and the oscillation frequency on (Figure 4.2) the droplet size and (Figure 4.3) size distribution under the amplitude of 6mm in the Span80/SDS emulsifier system

Figure 4.3 illustrates the coefficient of variation (CV) of droplets changes with the oscillation frequency under different oil phase fluxes. The curves all show the concave shape with a minimum point which indicates the optimal frequency with regard to the droplet size uniformity. The CV is in the range of 33% to 43%. The trend coincides with that in the distribution profile (Figure 4.1). It is noted that the optimal frequency depends on the dispersed phase flux, 6.3Hz for $8.3\times10^{-6}\,m^3/(m^2\cdot s)$, 8.4Hz for $13.8\times10^{-6}m^3/(m^2\cdot s)$ and 10.5Hz for $19.4\times10^{-6}m^3/(m^2\cdot s)$. Droplets coalescence, which can be observed on the micro-screen surface, happened when the frequency was smaller than the optimal frequency. Droplets grow bigger in the low shear stress and they are likely to touch and combine at the neighboring pores, which results in the larger CV values. After the optimal frequency, the CV increases with the increase in frequency. It is speculated that vortices in the continuous phase might appear under such high frequency condition. The droplet breakage within the vortices leads to the increase of CV.

Figures 4.4 and 4.5 show the droplet size and the size distribution vary as a function of the oscillation frequency under different oscillation amplitudes. Here the oscillation frequency limitation should be mentioned. The lowest oscillation frequency is 4.2Hz due to the mechanical frictional resistance. The highest oscillation frequencies are 12.6Hz, 20.9Hz and 25.1Hz for the amplitudes of 2mm, 6mm and 10mm correspondingly. The upper limitations are set for the stability of apparatus. As shown in Figure 4.4, the droplet size decreases with the frequency increasing. The changing trend stays the same as that in Figure 4.2. For the same frequency, the size of droplets prepared under the 2mm amplitude is the largest and that of the 10mm amplitude is the lowest as a result of the difference in shear stress. The CV of droplets is presented in Figure 4.5. Because of the higher shear stress that the 10mm amplitude can create, the optimal frequency with CV of 32% is the lowest frequency. Under the amplitude of 2mm, the optimal frequency is 18.9Hz with CV of 32%, in contrast with 8.4Hz with CV of 33% under the 6mm amplitude. The droplet coalescence and the water phase turbulence are the explanations as well for these phenomena.
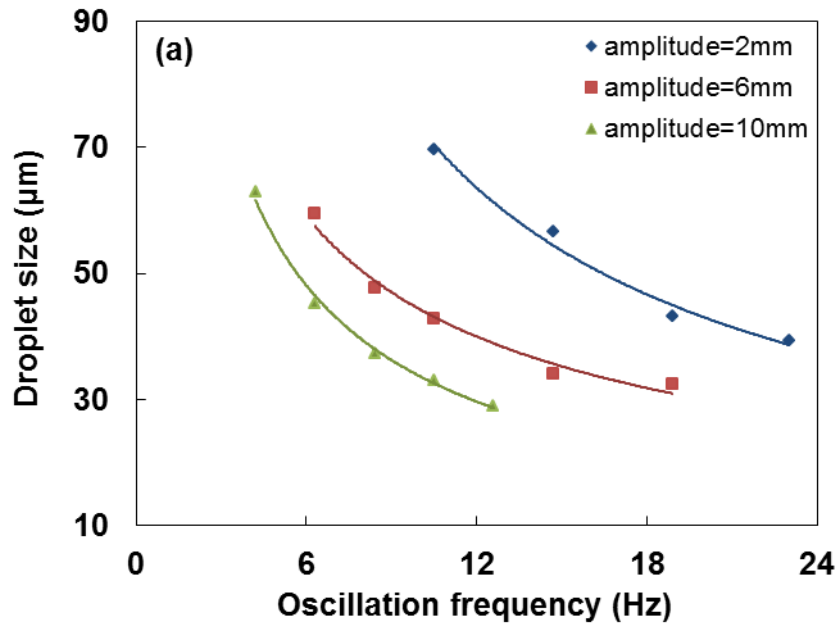
Figure 4.4
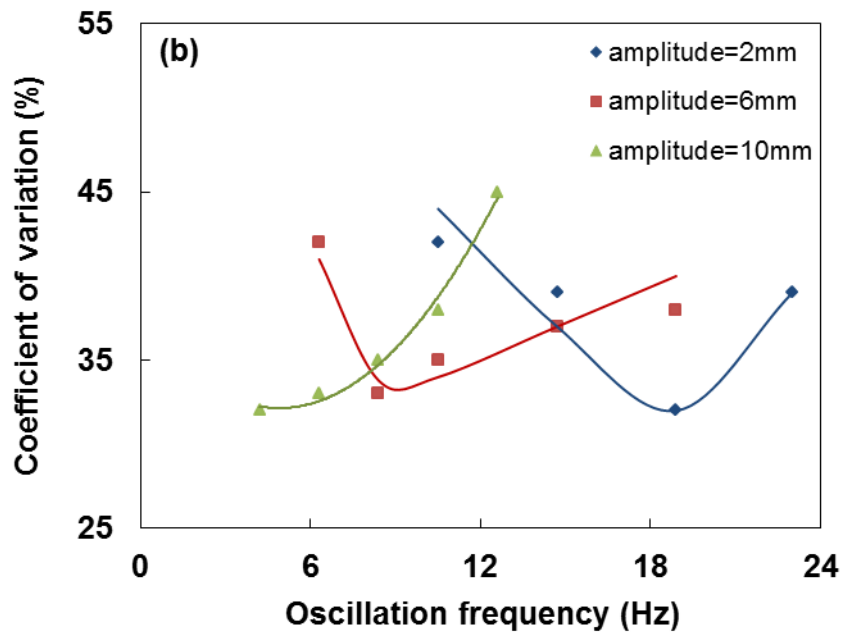
Figure 4.5

Effects of the oscillation amplitude and frequency on (Figure 4.4) the droplet size and (Figure 4.5) the size distribution using the same flux of $13.8×10^{-6} m^3/(m^2·s)$ in the Span80/SDS emulsifier system

Experimental evidence (Nakashima, Shimizu et al. 1991) showed that the average droplet size could be related to the average pore size by a linear relationship:

$$\overline{D_d} = k\,\overline{D_p} \tag{4.1}$$

where

$\overline{D_d}$ is the average diameter of droplets,

$\overline{D_p}$ is the average diameter of micro-screen pores,

and k is a constant for particular conditions.

The value of k is typically in the range of 2 to 10. In the figures shown above, however, the values of k sometimes are smaller than 2. In some cases, they are even smaller than one.

Using the high speed camera, it was possible to observe the lateral vibration of the oscillatory module. The vibration was found to have 1mm amplitude under the veridical oscillation amplitude of 10mm. The lateral vibration amplitude became smaller till undetectable with the oscillation amplitude reducing to 2mm. Although the lateral vibration was not obvious, the motion could facilitate droplets detaching from the micro-screen surface.

4.2 Effects of emulsifiers

For the micro-screen used in the apparatus with small space between pores, the appropriate choice of emulsifier is of importance for the success of membrane emulsification. The emulsifier should diffuse and adsorb rapidly to the newly formed oil/water interface to prevent droplets from coalescence between two adjacent pores. The emulsification in this system using 4%w/v Tween20 emulsifier system was not successful where the oil coalescence on the micro-screen surface was observed, particularly at small amplitudes and/or low frequencies. The emulsion throughput was low and a large part of oil formed a layer on the water surface. Therefore, the high throughput membrane emulsification requires the emulsifiers with fast adsorption dynamics. The bi-emulsifier system was considered (Wagdare, Marcelis et al. 2010). Span80 was chosen as the emulsifier in the oil phase to ensure the immediate availability of emulsifier molecules at the forming interfaces.
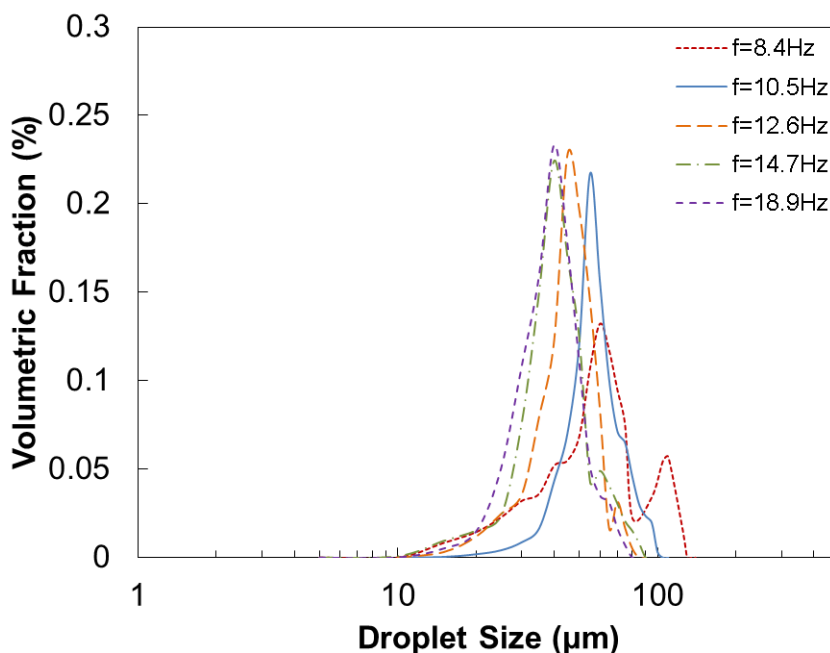
Figure 4.6 Droplet size distribution profile obtained in Span80/Tween20 system under oil phase flux=13.8×10^{-6}m^3/(m^2·s) and amplitude=6mm

The same experiments were repeated in the Span80(4%w/v)/Tween20(4%w/v) bi-emulsifier system. Figure 4.6 shows the droplet size distribution profile obtained in Span80/Tween20 system under oil phase flux of $13.8{\times}10^{-6}m^3/(m^2{\cdot}s)$ and amplitude of 6mm. It is shown that the average droplet size decreases with the frequency increasing. At the start frequency of 8.4Hz, the droplet size distribution is bad with two peaks appearing on the curve. The peak in the larger size region indicates coalescence of droplets. After then, the size distributions become narrow. By carefully comparing the distribution curves from 10.5Hz to 18.9Hz, the width of curve keeps approximate constant.

In figure 4.7, the average droplet size decreases with the increase in oscillation frequency. By comparison, the average size of droplets prepared in the Span80/Tween20 system is larger than that of droplets prepared in the Span80/SDS system at the same frequency. This is because the interfacial tension at the O/W interface in the Span80/Tween20 system is larger than that in the Span80/SDS system. The interfacial tension proportionally decides the capillary force which acts as a resistance to keep droplets attaching on micro-screen. Thus, the droplet needs to grow bigger to provide larger shear force to leave the micro-screen surface. On the other hand, Tween20 ($C_{58}H_{114}O_{26}$) has a larger molecular weight than that of SDS ($NaC_{12}H_{25}SO_4$) but a slower adsorption dynamics. So Tween20 molecules cannot adsorb onto the O/W interface as rapidly as SDS did. Slight coalescence should occur consequently. This explanation is proven by experimental evidence.
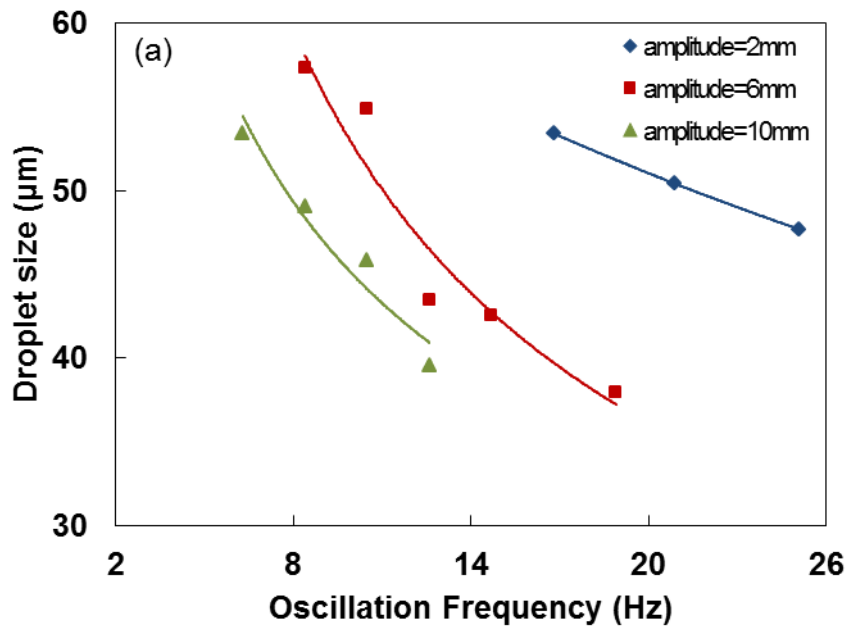
Figure 4.7
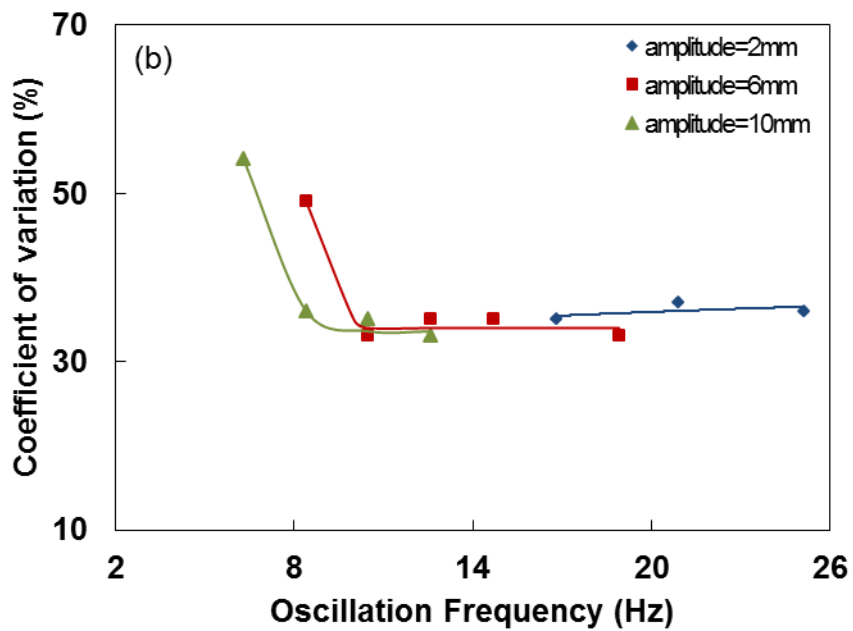
Figure 4.8

The variation of (Figure 4.7) the droplet size and (Figure 4.8) the size distribution as a function of the oscillation frequency and amplitude using the oil phase flux of 13.8×10⁻⁶m³/(m²·s) in the Span80/Tween20 emulsifier system

The starting frequencies (from this frequency emulsions can be produced efficiently) of the Span80/Tween20 system are greater than those of the Span80/SDS system by 2~4Hz. For instance, the starting frequency under the amplitude of 2mm in Span80/Tween20 is 16.8Hz as the comparison of 10.5Hz in Span80/SDS. As shown in Figure 4.8, the CV curves start with high values, but decrease rapidly to low values round 35% and keep stable with the frequency increasing. This trend coincides with that in the distribution profile (Figure 4.6). This means that the droplets in the Span80/Tween20 system are not so sensitive to the process parameters as those in the Span80/SDS system resulting from the larger interfacial intension.

Figures 4.9(a) and 4.9(b) present the optical micrographs of prepared emulsions. The average size of droplets in Figure 4.9(a) is 47.68μm with CV of 33%. The average size of droplets in Figure 4.9(b) is 54.88μm with CV of 33%.
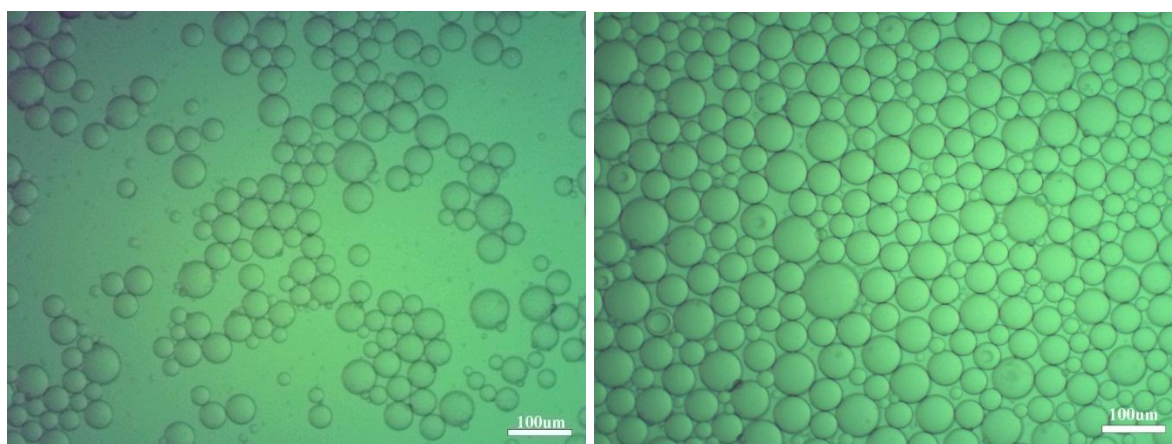
(a)   (b)

Figure 4.9 Optical micrographs of droplets.
(a) amplitude=6mm, frequency=8.4Hz and oil phase flux=13.8×10^{-6}m^3/(m^2·s)
in the Span80/SDS system
(b) amplitude=6mm, frequency=10.5Hz
and oil phase flux=13.8×10^{-6}m^3/(m^2·s) in the Span80/Tween20 system

Because of the droplet stability that the Span80/Tween20 system can provide, the oil phase flux can be largely increased under a high frequency. The maximum throughputs have been found at each highest frequency of the three amplitudes, as shown in Table 4.1.

The CV of approximately 50% has been considered as a limit for emulsion quality in industry. The dispersed phase maximum fluxes achieved in this system are considerably larger than the value of $92.5\times10^{-6} \text{m}^3/(\text{m}^2\cdot\text{s})$ reported for high porosity micro-screen-based cross-flow emulsification (Wagdare, Marcelis et al. 2010).

Table 4.1   Maximum fluxes achieved in the Span80/Tween20 emulsifier system

Amplitude/mm	Frequency/Hz	Flux/m^3/(m^2·s)	Average diameter/μm
2	25.1	200×10^{-6}	79.0
6	20.9	750×10^{-6}	37.1
10	12.6	400×10^{-6}	36.7

4.3   Effects of shear stress

The relationship between the droplet size and the shear stress has been explored. The shear stress (τ), for a Newtonian fluid, at a surface parallel to a flat plate, at the point y, is given by:

$$\tau_{(y)} = \mu \frac{\partial V}{\partial y}$$

(4.2)

where

μ is the viscosity of continuous phase,

V is the relative velocity of continuous phase along the boundary at the point with distance of y from the micro-screen surface.

y is the distance from the micro-screen surface.

Assuming laminar flow condition prevails, the relative velocity of continuous phase can be expressed in the term of the distance from the surface y by the well-known Stokes solution (Schlichting 1960):

$$V = V_o \left[1 - e^{-y/\delta_s} \cos(\omega t - y/\delta_s) \right]$$

(4.3)

where

V is the relative velocity of continuous phase at the point with distance of y from the micro-screen surface.

V_0 is the maximum relative velocity of continuous phase which equals to $V_{M,0}$, given by

$$V_0 = V_{M,0} = 4\sqrt{2}af$$

(4.4)

δ_s is the Stokes layer length given by

$$\delta_s = \sqrt{\frac{2v}{\omega}}$$

(4.5)

where

v is the kinematic viscosity of continuous phase.

Differentiating the Equation (4.2) after the substitution of V with Equation (4.3), the maximum shear stress can be obtained by the equation:

$$\tau = a\omega^{1.5} \rho v^{0.5}$$

(4.6)
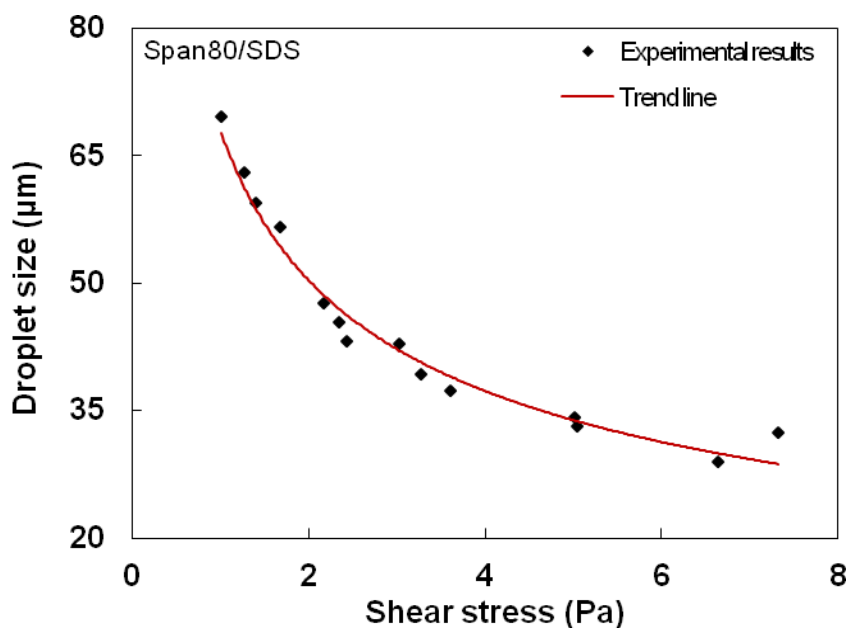
Figure 4.10 The relationship between the droplet size and the shear stress in the Span80/SDS system

Figure 4.10 shows that the droplet size varies as a function of shear stress. The droplet size experimental data can be fitted as a power function $D_d = 67.93\tau^{-0.43}$, which R^2=0.97. It is reasonable that the droplet diameter decreases with the shear stress increasing. And the droplet size decreasing rate becomes slow at the high frequency region due to the limitation of the micro-screen pore size.
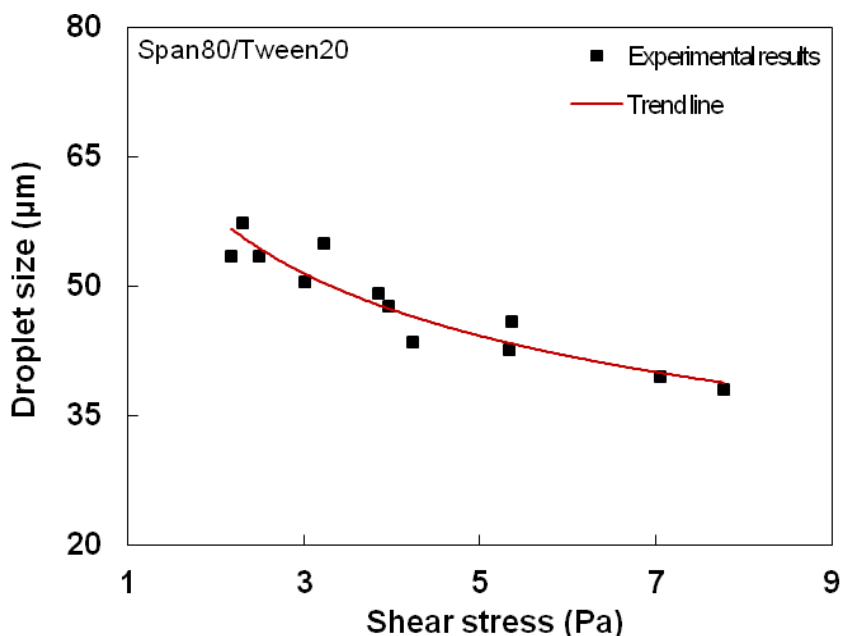
**Figure 4.11   The relationship between the droplet size and the shear stress
in the Span80/Tween20 system**

The size of droplet prepared in the Span80/Tween20 system also has been associated with shear stress calculated by Equation (4.5), as shown in Figure 4.11. The droplet size changes with shear stress as the same trend as that in the Span80/SDS system. Another power function ($D_d = 71.26\tau^{-0.30}$) best fits the experimental data as well, which can be concluded that the power and the factor of the regression function are related with the ingredients and concentrations of emulsifiers. However, the fitness of the power function (R^2=0.89) is not as good as that in the Span80/SDS system as the result of the emulsifier's properties. As discussed in the last section, the coalescence of droplets happened due to the slower adsorption dynamics of Tween20. The relative higher interfacial tension made the droplets stabilized by Span80/Tween20 insensitive to the shear stress.

4.4 Summary

The emulsion droplets show an average size ranging from 30μm to 70μm prepared through a stainless steel wire woven micro-screen with 30.5μm pore size under various process conditions.

A bi-emulsifier system is required to provide the fast adsorption dynamics. It is aimed to improve the droplet size uniformity, since the newly formed O/W interface can be covered by emulsifier molecules to prevent coalescence. The content of emulsifier system is found to affect the droplet size and uniformity due to different adsorption dynamics and interfacial tensions. The droplet size in the Span80/Tween20 system is larger than that in the Span80/SDS system under the same oil flux, amplitude and frequency. The uniformity of droplets in the Span80/SDS system becomes worse as the frequency increasing, while the uniformity of droplets in the Span80/Tween20 system keeps constant.

The droplet size is demonstrated to depend on the oscillation amplitude, frequency and micro-screen pore size. The dispersed phase flux does not influence the droplet size significantly in this system. The best size coefficient of variation (CV) is around 30%, which indicate the optimal oscillation frequency. The droplet uniformity will become worse due to coalescence or turbulence, if the oscillation frequency becomes either lower or higher.

To explore higher emulsification throughput, the micro-screen with the porosity of 36% was used as membrane. The oil phase maximum flux ($750 \times 10^{-6} m^3/m^2 \cdot s$) achieved in the Span80/Tween20 system is considerably larger than the value of $92.5 \times 10^{-6} m^3/m^2 \cdot s$ reported of the high porosity micro-screen-based cross-flow emulsification.

Chapter 5 Theory and modeling

5.1 Forces acting on a droplet

The membrane emulsification process can be divided into two stages theoretically, which are the droplet growth stage and the droplet detachment stage. In the growth stage, droplets are inflated from micro-screen pores and grow up. When a droplet is large enough, it tends to disconnect with the dispersed phase and snap off micro-screen in the detachment stage. The droplet size can be predicted on a single droplet in the detachment stage by a force balance.
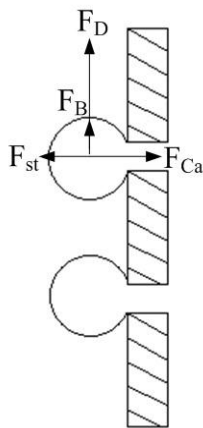
Figure 5.1   The framework of all forces applied on a single droplet

The forces exerted on a growing droplet have been investigated by many researchers (Peng and Williams 1998; Egidi, Gasparini et al. 2008; Hao, Gong et al. 2008). Figure 5.1 presents the framework of all forces acting on a single droplet forming at the tip of micro-screen pore. The main forces acting on a growing droplet from porous surface are the capillary force (F_{Ca}) due to interfacial tension, and the opposing drag force (F_D) caused by shear stress.

The capillary force is

$$F_{Ca} = \pi D_p \gamma \qquad (5.1)$$

where

D_p is the equivalent diameter of micro-screen rectangular pore,

γ is the interfacial tension on the interface of the dispersed phase and continuous phase. The data have been measured, as shown in Table D.1.

The drag force (F_D) caused by the continuous phase flow can be estimated based on the Stokes expression for Newtonian fluid:

$$F_D = 3\pi k_x \mu D_d V_d \qquad (5.2)$$

where

k_x is the wall correction factor given by O' Neil (O'Neil 1964) equals to 1.7 for a single sphere touching an impermeable wall within simple shear,

μ is the viscosity of continuous phase,

D_d is the droplet diameter,

V_d is the relative velocity between droplet and continuous phase at $y = D_d/2$. It can be obtained by equation (5.6) in Section 5.2.

Due to the "neck" between the forming drop and the micro-screen pore, a static force term F_{st} that accounts for the pressure difference between the inside and outside of the droplet is introduced, which would have an opposite sign to the capillary force (Egidi, Gasparini et al. 2008):

$$F_{st} = \frac{\gamma \pi}{D_d} D_p^2 \qquad (5.3)$$

When the droplets become close to the pore diameter, Equation (5.3) considering the neck underestimates the net capillary force, and the static force is no longer applicable.

The buoyancy (F_B) is

$$F_B = \frac{1}{6}\pi D_d^3 \left(\rho_c - \rho_d\right)g \tag{5.4}$$

where

ρ_c is the density of continuous phase,

ρ_d is the density of dispersed phase.

5.2 Oscillatory motion

For a surface placed in a fluid oscillating harmonically with an oscillation amplitude a, and an angular frequency ω, the velocity is

$$V_M = V_{M,0}\cos\omega t \tag{5.5}$$

where

ω equals to $2\pi f$,

V_M is the velocity of micro-screen at time t,

$V_{M,0}$ is the maximum velocity of micro-screen in the harmonic oscillation, given by

$$V_{M,0} = 4\sqrt{2}af \tag{4.4}$$

.

Assuming laminar flow condition prevails, the continuous phase velocity (relative velocity) can be expressed in terms of the distance from the surface y by the well-known Stokes solution (Schlichting 1960):

$$V = V_0 \left[1 - e^{-y/\delta_s} \cos(\omega t - y/\delta_s) \right]$$

$$(4.3)$$

where

V is the relative velocity of continuous phase at the point with distance of y from the micro-screen surface.

V_0 is the maximum relative velocity of continuous phase which equals to $V_{M,0}$.

δ_s is the Stokes layer length given by

$$\delta_s = \sqrt{\frac{2v}{\omega}}$$

$$(4.5)$$

where

v is the kinematic viscosity of continuous phase.

Equation (4.3) can be used to find out V_d which is the relative velocity between droplet and continuous phase at $y = D_d/2$. Thus, Equation (4.3) can be written as:

$$V_d = V_{M,0} \left[1 - e^{-y/\delta_s} \cos(\omega t - y/\delta_s) \right]$$

$$(5.6)$$

The relative velocity between droplet and continuous phase changes as the cosine function. For simplication, the average value ($\sqrt{2}/2$) of cosine function has been adopted here.

Finally, in the capillary force (F_{Ca}), the drag force (F_D), the static force (F_{st}) and the buoyancy (F_B), droplet diameter (D_d) is the only variable needed to be determine.

5.3 Torque balance and force balance

If the droplet keeps approximate sphere during the detachment stage, the droplet size can be predicted by a torque balance. The forces shown in Figure 5.1 can be sorted into two groups. The drag force and buoyancy act as the detachment torque. The capillary force and the static force act as the attachment torque:

$$\left(F_D + F_B \right) h = \left(F_{Ca} + F_{st} \right) \frac{D_p}{2}$$

(5.7)

where

h is the distance from the micro-screen surface to the top of droplet, which can be calculated in respect of geometry:
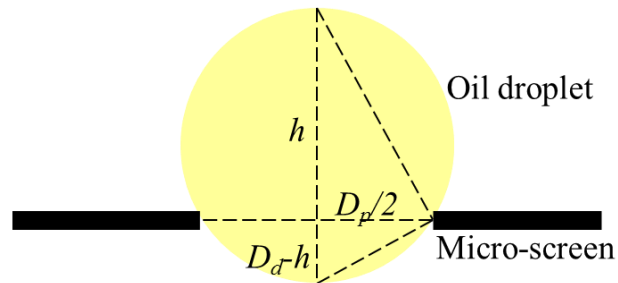
$$\frac{h}{D_p/2} = \frac{D_p/2}{D_d - h}$$

(5.8)

If the droplet deforms severely in the detachment stage, a force balance can be applied to estimate the droplet size by

$$F_D + F_B = F_{Ca}$$

(5.9)

As the oscillatory micro-screen emulsification is an intense process, the detachment stage takes a very short time. It is assume that the dispersed phase flux does not virtually affect the droplet size based on a rational simplication. This assumption also is verified by the experimental data in Section 4.1.

5.4 Model solution

The parameters: pore diameter (D_p), amplitude (a), frequency (f), distance from the micro-screen surface to the top of droplet (h), wall correction factor (k_x), interfacial tension on the interface of the dispersed phase and continuous phase (γ), viscosity of continuous phase (μ), kinematic viscosity of continuous phase (v), density of continuous phase (ρ_c), density of dispersed phase (ρ_d) are known.

The average droplet size can be calculated by the following equations:

$$F_{Ca} = \pi D_p \gamma \tag{5.1}$$

$$F_D = 3\pi k_x \mu D_d V_d \tag{5.2}$$

where $V_d = V_{M,0}\left[1 - e^{-y/\delta_s}\cos(\omega t - y/\delta_s)\right]$, $\delta_s = \sqrt{\dfrac{2v}{\omega}}$, $\omega = 2\pi f$,

$$F_{st} = \frac{\gamma\pi}{D_d} D_p^2 \tag{5.3}$$

$$F_B = \frac{1}{6}\pi D_d^3 \left(\rho_c - \rho_d\right)g \tag{5.4}$$

$$\left(F_D + F_B\right)h = \left(F_{Ca} + F_{st}\right)\frac{D_p}{2} \tag{5.7}$$

where $$\frac{h}{D_p/2} = \frac{D_p/2}{D_d - h} \tag{5.8}$$

or $$F_D + F_B = F_{Ca} \tag{5.9}$$

The droplet size can be obtained by solving the above six equations above which includes six variables.

5.5 Comparisons between modeling and experimental results

The torque balance model and the force balance model have been tested in both the Span80/SDS system and the Span80/Tween20 system. The comparisons of modeling results and experimental data are presented in Figure 5.2 and Figure 5.3.
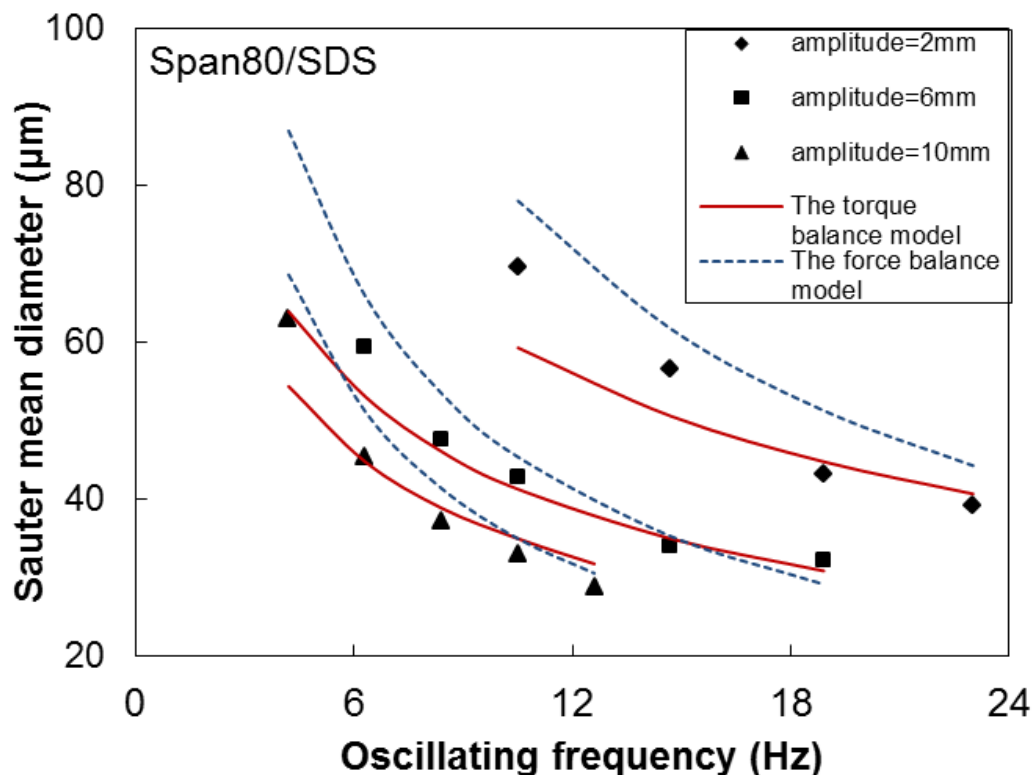
Figure 5.2 The comparison of experimental data and modeling results in the Span80/SDS system

The experimental results show that the droplet sizes are in the region close to the micro-screen pore diameter ($D_d < 2D_p$). Hence, the static force (F_{st}) can be neglected (Egidi, Gasparini et al. 2008). The modeling results did evidence this. Figure 5.2 presents the experimental results, the modeling curves from the torque balance model and the force balance model. It easily can be seen that the torque balance model fits the experimental results well, nevertheless the force balance does not. Therefore, the torque balance model

is more suitable for the oscillatory micro-screen system. Due to coalescence of droplets in the starting frequency region, the first several experimental results are larger than the modeling results.
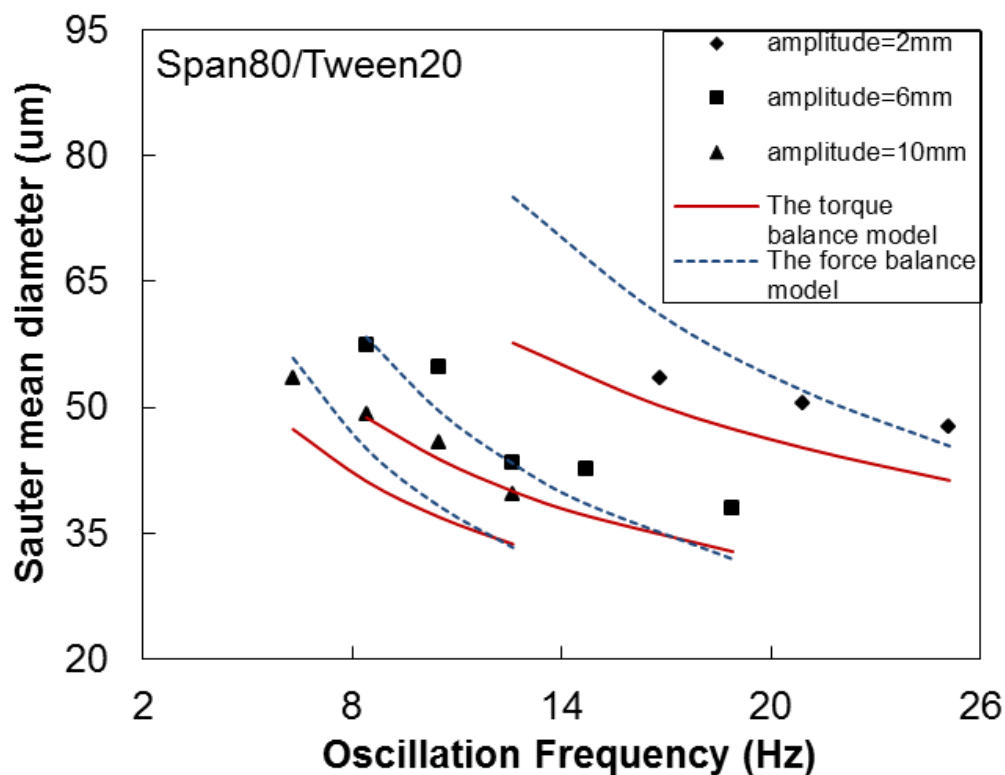
Figure 5.3   The comparison of experimental data and modeling results in the Span80/Tween20 system

However, in the Span80/Tween20 system, both models cannot work (shown in Figure 5.3). The experimental data are basically larger than the modeling results. It is probably because the droplet coalescence happens during the emulsification process.

5.6 Summary

The droplet formation mechanism in the oscillatory micro-screen emulsification is introduced in this chapter. The torque balance model and the force balance model have been developed from the forces analysis on a single forming droplet in the detachment stage. The average droplet size can be calculated by iterative method.

By comparing two models and the experimental data, it is found that the torque balance can better predict the average droplet size. Therefore, we understand that growing droplets keep approximate sphere during detaching. The torque balance model fits the experimental data well in the Span80/SDS system, because the droplets in this system are more sensitive to the changes of process conditions. In contrast, the model fails in the Span80/Tween20 system, because unpredictable droplet coalescence happens on the micro-screen surface. Thus, it is concluded that average droplet size can be predicted in the emulsifier system with fast diffusion and adsorption dynamics.

Chapter 6 Effects of channel geometries on emulsion quality

In this chapter, the width of continuous phase container was narrowed by attaching inserts on both walls facing micro-screens. Three types of insert with different surface geometries, such as the flat, the wavy and the surface with baffle plates, have been investigated in the Span80/SDS system. It was aimed to see whether possibly formed eddies would break large droplets into small ones and improve the emulsion uniformity consequently.

6.1   Effects of the channel with flat surface

The distance between the flat surface of insert and the micro-screen surface was reduced to 2mm. The original width between the micro-screen surface and the container wall is 30mm. Systematic experiments were carried out under different oscillation amplitudes by changing oscillation frequencies. Figure 6.1 shows the comparison of the droplet sizes in the container with original width and those in the container with flat inserts. The droplet size decreases with the increasing of oscillation frequency under each amplitude with the same trend. However, it is easily seen that the droplet sizes are all significantly reduced in the narrower channel.
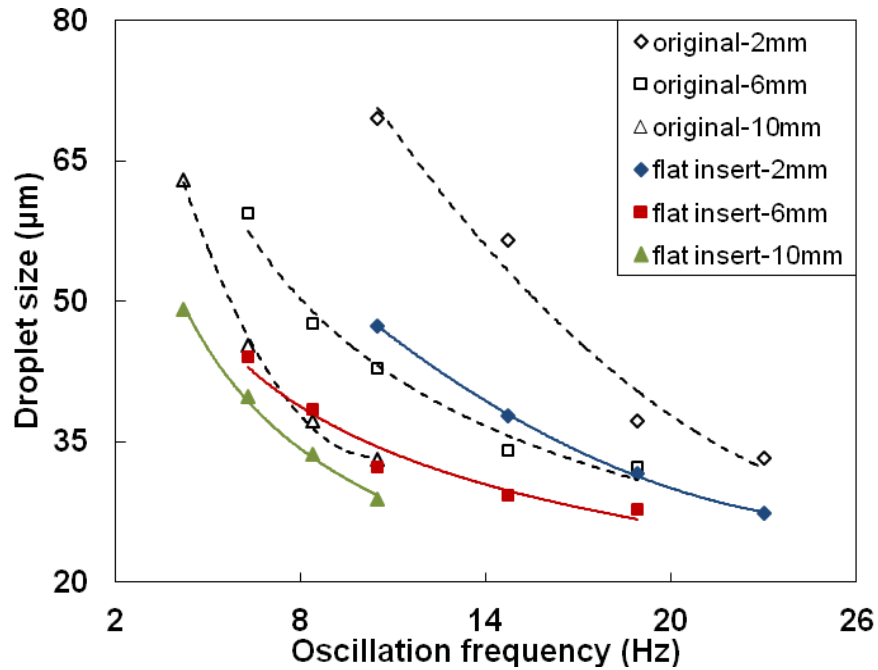
Figure 6.1

Figure 6.2

The comparisons of (Figure 6.1) the droplet sizes and (Figure 6.2) the size distributions in the original container and the results in the container with flat inserts
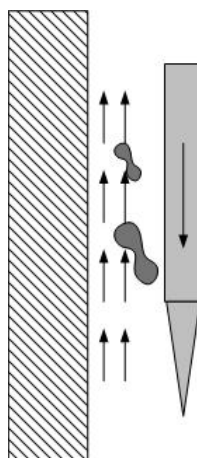
Figure 6.3   Schematic illustration of the effect of hydrodynamic pressure on the droplet size in the container with flat inserts

It is speculated that droplets would rupture after leaving the micro-screen surface, which leads to the size reduction. Because of the oscillatory motion of the micro-screen module, the counter flow caused by the inertial force applies a higher shear force on a growing droplet (illustrated in Figure 6.3). The hydrodynamic pressure of the continuous phase deforms droplets and further breaks them into more fragments. Moreover, the differences of droplet size between the two conditions are larger at the few beginning frequencies, since the large droplets in this region are more likely to deform. It is also interestingly found that the droplet sizes obtained in the narrower channel are no larger than 50μm and several of them even smaller than the micro-screen pore size (30.5μm). In contrast, the continuous phase stays stagnantly around the micro-screen module in the original container without inserts. The hydrodynamics has no influence on the droplet size.

Figure 6.2 shows the comparison of the size coefficient of variation (CV) in the original container and that in the container with flat inserts. It is seen that the CVs in the both conditions have the similar changing trend, but the CVs obtained in the container with flat inserts all become larger, which means the droplet size distributions become wider. Therefore, the narrow width of the continuous phase channel is a negative effect in the respect of the droplet size uniformity because of the uncontrollable droplet breakage

caused by the cross flow in the continuous phase. It is also found that the differences in CV become larger and larger from the low frequency region to the higher frequency region. It is demonstrated that the higher oscillation frequency the more severe cross flow is. Moreover, very small satellite droplets turn up in the process of droplet breakage, as presented in Figure 6.4. And it is more possible to generate the satellite droplets when the interfacial tension is low. The small satellite droplets with the size of 3~5μm can be found in the micrograph (shown in Figure 6.5).
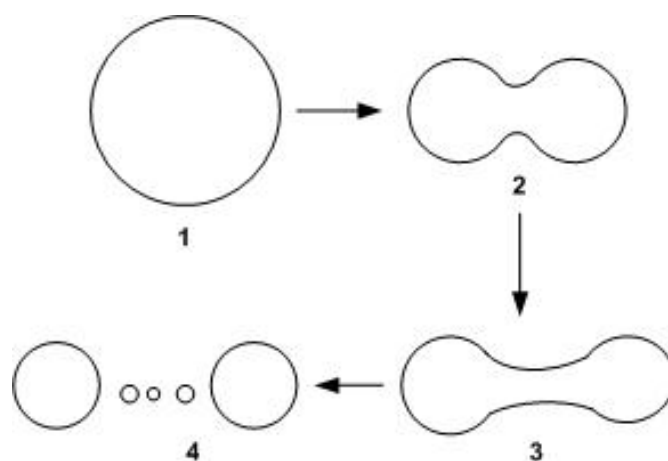
Figure 6.4   Schematic illustration of the droplet breakage process
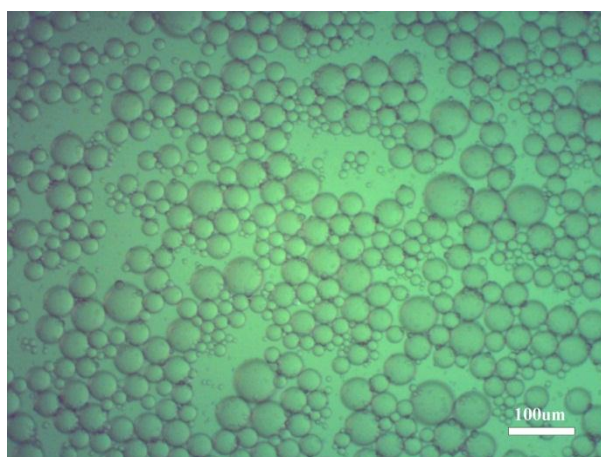
**Figure 6.5   Micrograph of the sample prepared in the container
with flat inserts**

6.2   Effects of the channel with wavy surface

The effects of the wavy surface on emulsion quality have been investigated in this section. The distance between the tip of wave to the micro-screen surface is 2mm. Figure 6.6 and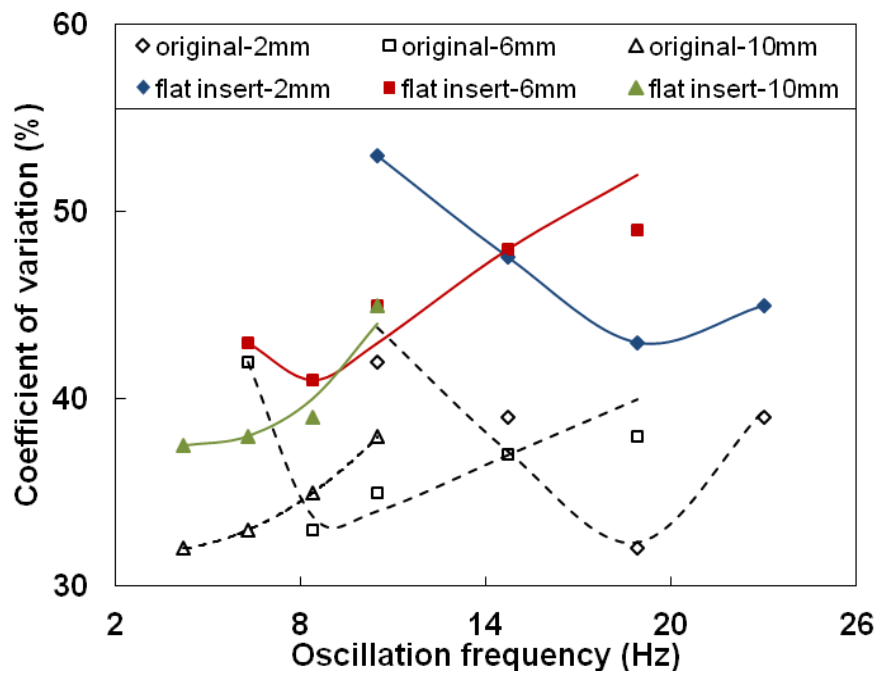 Figure 6.7 show the comparisons of the droplet sizes and the size distributions in the original container and the results in the container with wavy inserts.

The similar results of the droplet size and the coefficient of variation can be found in the container with wavy inserts as those in the container with flat inserts. It is demonstrated that the cross flow still exists but the wavy surface is unable to strengthen the cross flow. For the wavy geometry with obtuse angles, the cross flow just travels attaching the surface so that no stronger eddies can be created to affect droplets, as shown in Figure 6.8.
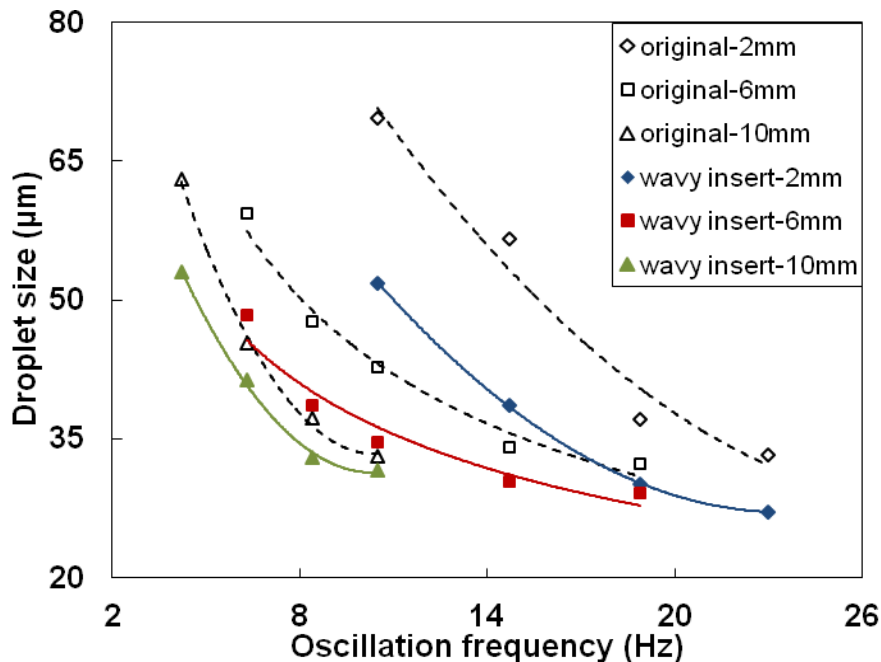
Figure 6.6   The comparison between the droplet sizes in the original container and those in the container with wavy inserts
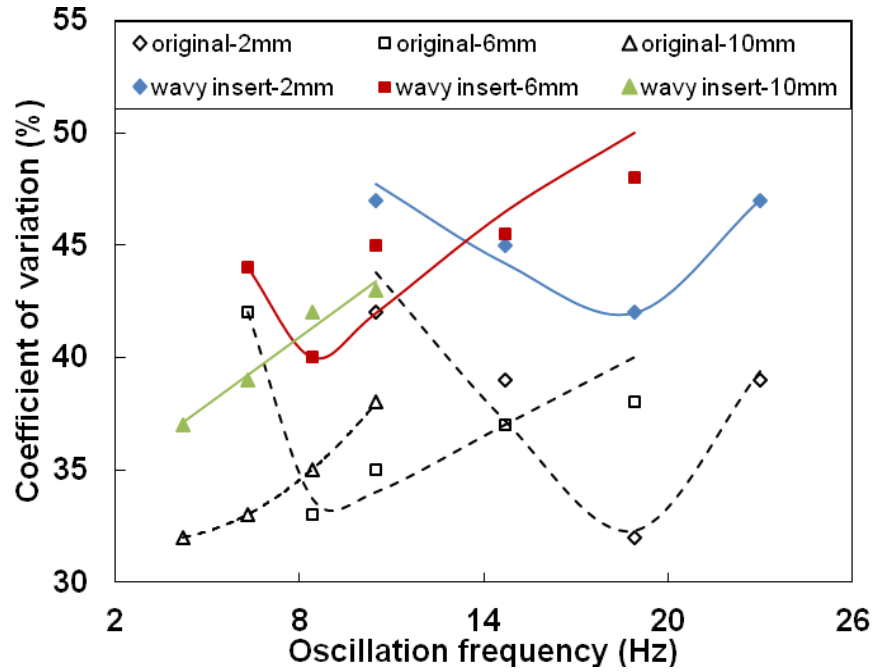
Figure 6.7   The comparison between the size distributions in the original container and those in the container with wavy inserts
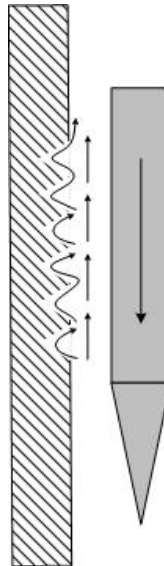
Figure 6.8   Schematic illustration of the cross-flow in the container with wavy inserts

6.3   Effects of the channel with baffles

Several pieces of iron plates were fixed on the insert surface standing 5mm high to play as baffles. The gap between two baffles is 16mm and the distance from the tip of baffle to the micro-screen surface is 2mm. The effects of baffles on the emulsion quality have been studied in this section.

Figure 6.9 shows the results of droplet size as a function of oscillation frequency in the container with baffles and the original container. The droplet size in both situations decreases with the oscillation frequency increasing. However, the droplet size affected by baffles is significantly reduced. The droplet sizes obtained in the container with baffles are no larger than 40µm and several of them are even smaller than the micro-screen pore size (30.5µm). It is demonstrated that the droplets also suffered breakage during the emulsification process. In this situation, eddies should be created resulting from the resistance of baffles to the continuous phase's cross flow. Eddies usually emerge beside the baffles, as illustrated in Figure 6.11. The droplets were disrupted in eddies by the viscous stress in the continuous phase, as shown in Figure 6.12. The difference of droplet size between the two situations becomes smaller and smaller under each oscillation amplitude. It is because the droplets are larger at the beginning frequencies and they are more prone to deform and break up, which leads to the increase of CV.
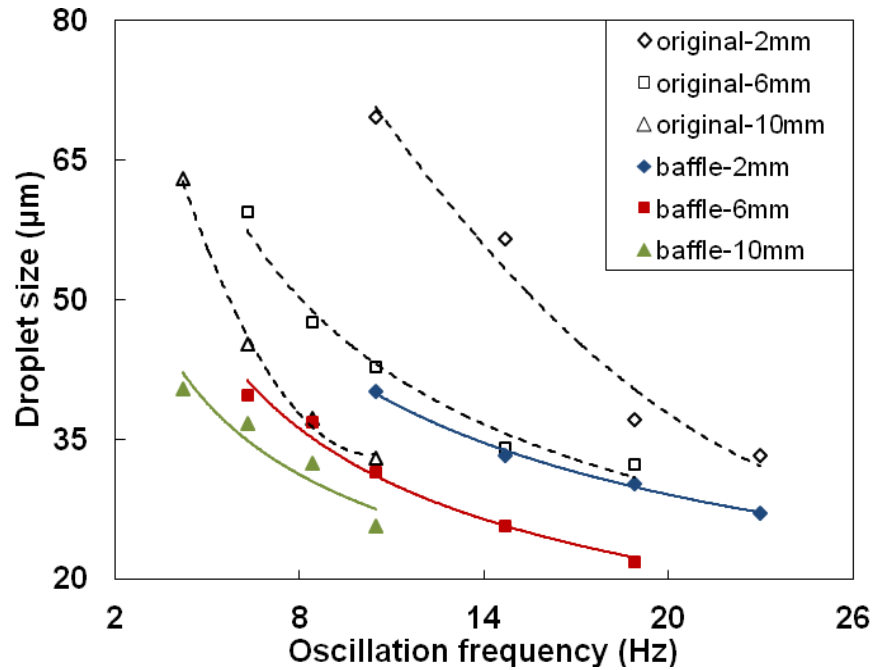
Figure 6.9
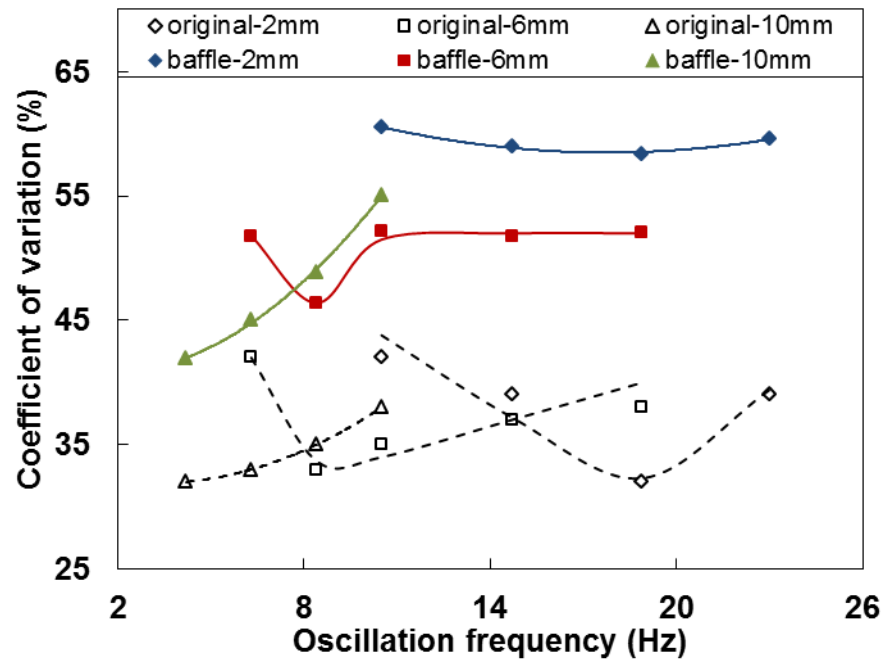
Figure 6.10

**The comparison of (Figure 6.9) the droplet size and (Figure 6.10) the size distribution in the original container
and the results in the container with baffles**
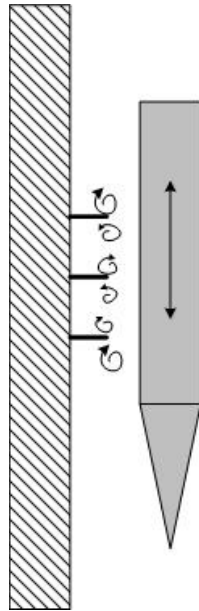
Figure 6.11 Schematic illustration of the eddies in the container with baffles on the inserts
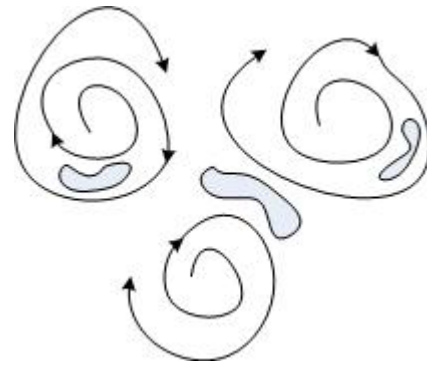
Figure 6.12 Schematic illustration of the droplet breakage process in eddies

Figure 6.10 shows the comparison of CV in the container with baffles and that in the original container. The CVs obtained in the container with baffles are at least 10% larger than those in the original container. Therefore, it is concluded that the insert surface with baffles is a negative effect as well in the regard of droplet size uniformity. For the oscillation amplitudes of 2mm and 6mm, the CVs become stable after the frequency reaching to 10Hz, which the CVs keep 52% under the amplitude of 6mm and 60% under the amplitude of 2mm. For the amplitude of 10mm, the CVs in the two situations show a similar trend which increases with frequency increasing.
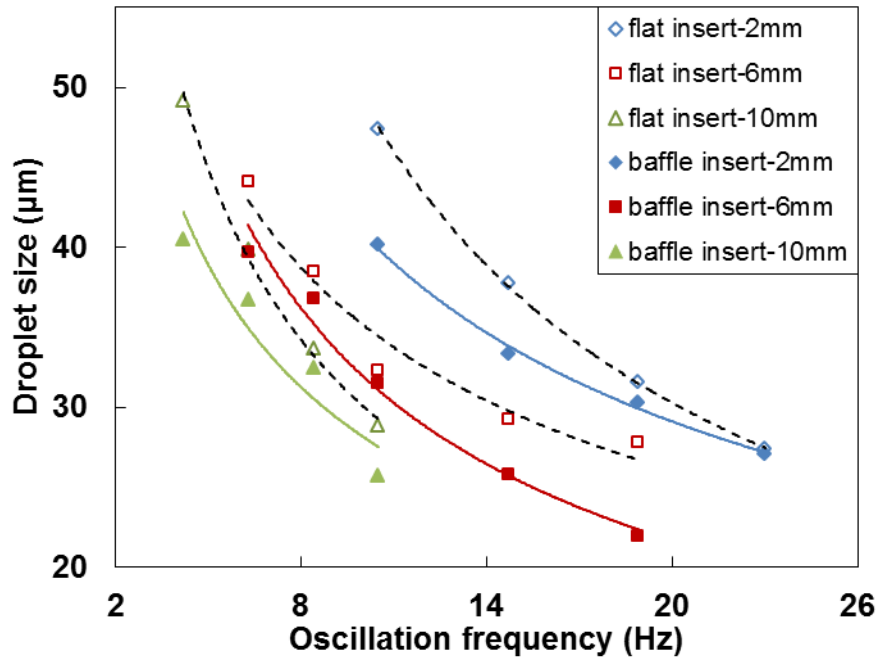
Figure 6.13
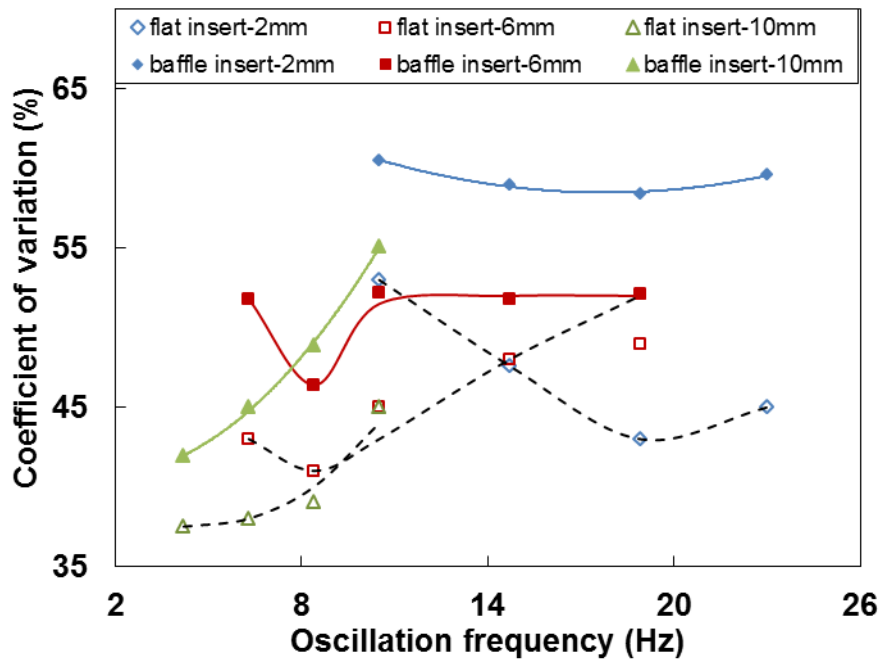
Figure 6.14

The comparisons of (Figure 6.13) the droplet size and (Figure 6.14) the size distribution in the original container and those in the container with baffles

Figure 6.13 and Figure 6.14 compare the droplet size and the CV obtained from the container with flat inserts with the results from the container with baffles. It is found that the baffles have more significant effects on emulsion quality than the flat inserts. The droplet size prepared with baffles is smaller, but the size uniformity is worse. It is demonstrated that eddies could create much stronger impacts on droplets than the cross flow.

6.4 Summary

In this chapter, the continuous phase channel geometries have been investigated. The flat inserts, the wavy inserts and the inserts with baffles were studied. The results show that the channel geometry and the narrow width (close to the boundary layer) between the micro-screen surface and the container wall have significant effects on the emulsion quality. The droplet size decreased and the size distribution became wider. With respect to monodispersion, the continuous phase channels with various geometries produce negative influences in the oscillatory micro-screen emulsification system. In order to improve the uniformity of emulsion products in this system, turbulence or eddies in the continuous phase should be avoided. However, the volume-adjustable container still can be applied in design, which is able to expand the production range in the droplet size.

Chapter 7 Conclusions and recommendations

7.1 Conclusions

A membrane emulsification system which utilizes oscillatory motion to generate shear stress for manufacturing emulsions is studied in this thesis. The emulsion droplets show an average size ranging from 30μm to 70μm prepared through a stainless steel wire woven micro-screen with 30.5μm pore size under various process conditions.

A bi-emulsifier system is required to provide the fast adsorption dynamics. It is aimed to improve the droplet size uniformity, since the newly formed O/W interface can be covered by emulsifier molecules to prevent coalescence. The content of emulsifier system is found to affect the droplet size and uniformity due to different adsorption dynamics and interfacial tensions. The droplet size in the Span80/Tween20 system is larger than that in the Span80/SDS system under the same oil flux, amplitude and frequency. The uniformity of droplets in the Span80/SDS system becomes worse as the frequency increased, while the uniformity of droplets in the Span80/Tween20 system keeps constant.

The droplet size is demonstrated to be influenced by the oscillation amplitude, frequency and micro-screen pore size. The dispersed phase flux does not influence the droplet size significantly in this system. The best size coefficient of variation (CV) is around 30%, where can indicate the optimal oscillation frequency. The droplet uniformity worsen due to coalescence or turbulence, if the oscillation frequency becomes either lower or higher.

To explore higher emulsification throughput, the micro-screen with the porosity of 36% was used as micro-screen. The oil phase maximum flux ($750 \times 10^{-6} m^3/m^2 \cdot s$) achieved in the Span80/Tween20 system is considerably larger than the value of $92.5 \times 10^{-6} m^3/m^2 \cdot s$ reported of the high porosity micro-screen-based cross-flow emulsification.

By analyzing the droplet formation process, the parameters like oscillation amplitude, frequency, continuous phase density and kinematic viscosity can be integrated into the

shear stress equation. Therefore, the droplet size data can be associated with the shear stress as a power function. Moreover, the droplet size can be predicted in the detachment stage using the torque balance model. The modeling results fit the experimental data well in the Span80/SDS system, because the droplets in this system are more sensitive to the changes of process conditions. In contrast, the model fails in the Span80/Tween20 system, because the coalescence of droplets happens on the micro-screen surface.

The insert surface geometries of the continuous phase container have been investigated. The flat inserts, the wavy inserts and the inserts with baffles were studied. The results show that the surface geometry and the narrow width (close to the boundary layer) between the micro-screen surface and the container wall have significant effects on the emulsion quality. The droplet size decreased and the size distribution became wider. With respect to monodispersion, the inserts with various geometries produce detrimental influences in the oscillatory micro-screen emulsification system. In order to improve the uniformity of emulsion products in this system, turbulence or eddies in the continuous phase should be avoided. However, the volume-adjustable container still can be applied in design, which is able to expand the production range in the droplet size.

7.2 Recommendations

Many characteristics of the oscillatory micro-screen emulsification system are needed to be investigated in the future. The following recommendations are given towards future work:

1. Different types of micro-screen had better be tested to explore the optimal porosity and the effects of pore opening shape.
2. The relationship between the ratio of active pores and the process conditions should be studied. The actual oil phase flux can be obtained if the ratio of active pores is known. This will provide data for a better prediction of the droplet size and number.
3. The oscillatory micro-screen emulsification can be combined with the premix process, which pushes the premixed emulsions going through the oscillatory micro-screen. Moreover, the repeated oscillatory emulsification process can be applied as well, which lets the prepared emulsions go through the oscillatory micro-screen several times. These two design are both promising in improving emulsion quality.
4. The multiple emulsions would be prepared in the oscillatory micro-screen emulsification system under mild process conditions. For example, the W/O/W multiple emulsions can be produced by two steps. Firstly, disperse the water phase into the oil phase to form the W/O emulsions. Then, repeat the micro-screen emulsification process by pushing the W/O emulsions into the water phase again.

References

Abraham, S., Eun Ho, J., et al. (2006). "Microfluidics assisted synthesis of well-defined spherical polymeric microcapsules and their utilization as potential encapsulants." Lab on a Chip 6(6): 752-756.

Abrahamse, A. J., Van der Padt, A., et al. (2001). "Process fundamentals of membrane emulsification: Simulation with CFD." AIChE Journal 47(6): 1285-1291.

Abrahamse, A. J., Van Lierop, R., et al. (2002). "Analysis of droplet formation and interactions during cross-flow membrane emulsification." Journal of Membrane Science 204(1-2): 125-137.

Aryanti, N., Hou, RZ., et al. (2009). "Performance of a rotating membrane emulsifier for production of coarse droplets." Journal of Membrane Science 326(1): 9-18.

Couvreur, P., Blanco-Prieto, M. J., et al. (1997). "Multiple emulsion technology for the design of microspheres containing peptides and oligopeptides." Advanced Drug Delivery Reviews 28(1): 85-96.

Vasiljevic, D., Parojcic, J., Primorac, M., Vuleta, G. (2006). "An investigation into the characteristics and drug release properties of multiple W/O/W emulsion systems containing low concentration of lipophilic polymeric emulsifier." International Journal of Pharmaceutics 309(1-2): 171-177.

Dragosavac, M. M., Sovilj, M. N., et al. (2008). "Controlled production of oil-in-water emulsions containing unrefined pumpkin seed oil using stirred cell membrane emulsification." Journal of Membrane Science 322(1): 178-188.

Dragosavac, MM., Holdich, RG., Vladisavljevic, GT., Sovilj, MN. (2012). "Stirred cell membrane emulsification for multiple emulsions containing unrefined pumpkin seed oil with uniform droplet size." Journal of Membrane Science 392-393: 122-129.

Egidi, E., Gasparini, G., et al. (2008). "Membrane emulsification using membranes of regular pore spacing: droplet size and uniformity in the presence of surface shear." Journal of Membrane Science 323(2): 414-420.

Gomaa, HG., Rao, S., Al-Taweel, AM., (2011). "Intensification of membrane microfiltration using oscillatory motion." Separation and Purification Technology 78: 336-344

Gao, F., Su, ZG., et al. (2009). "Double emulsion templated microcapsules with single hollow cavities and thickness-controllable shells." Langmuir 25(6): 3832-3838.

Garstecki, P., Fuerstman, M. J., et al. (2006). "Formation of droplets and bubbles in a microfluidic T-junction - scaling and mechanism of break-up." Lab on a Chip 6(3): 437-446.

Gijsbertsen-Abrahamse, A. J., Van Der Padt, A., et al. (2004). "Status of cross-flow membrane emulsification and outlook for industrial application." Journal of Membrane Science 230(1-2): 149-159.

Okochi, H., Nakano, M. (1997). "Comparative study of two preparation methods of w/o/w emulsions: stirring and membrane emulsification." Chem. Pharm. Bull 45: 1323-1326.

Hao, DX., Gong, FL., et al. (2008). Controlling factors on droplets uniformity in membrane emulsification: Experiment and modeling analysis, Industrial & Engineering Chemistry Research 47(17): 6418-6425

Holdich, RG., Dragosavac, MM., Vladisavljevic, GT., Kosvintsev, SR. (2010). "Membrane emulsification with oscillating and stationary membranes." Industrial & Engineering Chemistry Research 49: 3810-3817.

Holdich, RG., Dragosavac, MM., Vladisavljevic, GT., Piacentini, E. (2013). "Continuous membrane emulsification with pulsed (oscillatory) flow." Industrial & Engineering Chemistry Research 52: 507-515.

Jager-Lezer, N., Terrisse, I., et al. (1997). "Influence of lipophilic surfactant on the release kinetics of water-soluble molecules entrapped in a W/O/W multiple emulsion." Journal of Controlled Release 45(1): 1-1.

Jiao, J., Rhodes D. G., et al. (2002). "Multiple emulsion stability: Pressure balance and interfacial film strength." Journal of Colloid and Interface Science 250(2): 444-450.

Joscelyne, S. M. and Tragardh, G. (2000). "Membrane emulsification - A literature review." Journal of Membrane Science 169(1): 107-117.

Kobayashi, I., Nakajima, M. et al. (2002). "Silicon array of elongated through-holes for monodisperse emulsion droplets." AIChE Journal 48(8): 1639-1644.

Kobayashi, I., Nakajima, M. et al. (2003). "Preparation characteristics of oil-in-water emulsions using differently charged surfactants in straight-through microchannel emulsification." Colloids and Surfaces A: Physicochemical and Engineering Aspects 229(1-3): 33-41.

Kosvintsev, S. R., Gasparini, G., et al. (2005). "Liquid - Liquid membrane dispersion in a stirred cell with and without controlled shear." Industrial and Engineering Chemistry Research 44(24): 9323-9330.

Lesmes, U. and McClements, D. J. (2009). "Structure-function relationships to guide rational design and fabrication of particulate food delivery systems." Trends in Food Science and Technology 20(10): 448-457.

Lingling, S., van den Berg, A., et al. (2009). "Interfacial tension controlled W/O and O/W 2-phase flows in microchannel." Lab on a Chip 9(6): 795-801.

Lobo, L., Svereika, A. et al. (2002). "Coalescence during emulsification. 1. Method development." Journal of Colloid and Interface Science 253(2): 409-418.

Lobo, L. and Svereika, A. (2003). "Coalescence during emulsification: 2. Role of small molecule surfactants." Journal of Colloid and Interface Science 261(2): 498-507.

McClements, D. J. (2012). "Advances in fabrication of emulsions with enhanced functionality using structural design principles." Current Opinion in Colloid and Interface Science 17(5): 235-245.

Mine, Y., Shimizu, M., et al. (1996). "Preparation and stabilization of simple and multiple emulsions using a microporous glass membrane." Colloids and Surfaces B: Biointerfaces 6(4-5): 261-261.

Muller, R. H., Radtke, M., et al. (2002). "Solid lipid nanoparticles (SLN) and nanostructured lipid carriers (NLC) in cosmetic and dermatological preparations", Advanced Drug Delivery Reviews 54(1): S131-S155

Nakashima, T., Shimizu, M., et al. (1991). "Membrane emulsification by microporous glass." Key Engineering Materials 61-62: 513-516.

O'Neil, M. E. (1964). "A slow motion of viscous liquid caused by a slowly moving solid sphere." Chem Eng Sci 23: 67-74.

Olivieri, L., Seiller, M., et al. (2003). "Optimization of a thermally reversible W/O/W multiple emulsion for shear-induced drug release." Journal of Controlled Release 88(3): 401-412.

P. Walstra, Smulders, P. E. A. (1998). "Emulsion formation, in: B.P. Binks (Ed.), Modern Aspects of Emulsion Science." The Royal Society of Chemistry, Cambridge: 56–99.

Pawlik, A. K. and Norton, I. T. (2012). "Encapsulation stability of duplex emulsions prepared with SPG cross-flow membrane, SPG rotating membrane and rotor-stator techniques-A comparison." Journal of Membrane Science 415-416: 459-468.

Peng, S. J. and Williams, R. A. (1998). "Controlled production of emulsions using a crossflow membrane. Part I: Droplet formation from a single pore." Chemical Engineering Research and Design 76(A8): 894-901.

Schlichting, H. (1960) "Boundary Layer Theory." McGraw-Hill, New York.

Schroder, V. (1999). Herstellen von Öl-in-Wasser-Emulsionen mit Mikroporösen Membranen PhD Thesis, Technische Hochschule Karlsruhe.

Schroder, V., Behrend, O., et al. (1998). "Effect of dynamic interfacial tension on the emulsification process using microporous, ceramic membranes." Journal of Colloid and Interface Science 202(2): 334-334.

Schubert, H. and Armbruster, H. (1992). "Principles of formation and stability of emulsions." International chemical engineering 32(1): 14-28.

Seo, M., Paquet, C., et al. (2007). "Microfluidic consecutive flow-focusing droplet generators." Soft Matter 3(8): 986-992.

Song, H., Chen, D. L., et al. (2006). "Reactions in droplets in microfluidic channels." Angewandte Chemie - International Edition 45(44): 7336-7356.

Soon, S. Y., Harbidge, J., et al. (2001). "Prediction of drop breakage in an ultra high velocity jet homogenizer." Journal of Chemical Engineering of Japan 34(5): 640-646.

Spyropoulosa, F., Hancocks, R. D., Norton I. T. (2011). "Food-grade emulsions prepared by membrane emulsification techniques." Procedia Food Science (1): 920-926.

Stang, M., Karbstein, H., et al. (1994). "Adsorption kinetics of emulsifiers at oil-water interfaces and their effect on mechanical emulsification." Chemical engineering and processing 33(5): 307-311.

Stillwell, M. T., Holdich, R. G., et al. (2007). "Stirred cell membrane emulsification and factors influencing dispersion drop size and uniformity." Industrial and Engineering Chemistry Research 46(3): 965-972.

Sugiura, S., Nakajima, M., et al. (2000). Formation of monodispersed microspheres from microfabricated channel array. 1st Annual International IEEE-EMBS Special Topic Conference on Microtechnologies in Medicine and Biology. Proceedings, 12-14 Oct. 2000, Piscataway, NJ, USA, IEEE.

Nakashima, T. (2002). Membrane and Particle Science and Technology in Food and Medical Care. History of SPG technology and its recent advances. Proc. 38th Int. SPG Forum. Miyazaki: 63.

Utada, A. S., Lorenceau, E., et al. (2005). "Monodisperse double emulsions generated from a microcapillary device." Science 308(5721): 537-541.

Schröder, V., Schubert, H. (1997). Emulsification using microporous, ceramic membranes. the First European Congress on Chemical Engineering (ECCE 1), Florence, Italy.

Schröder, V., Wang, Z., Schubert, H. (1997). Production of oil-in-water emulsions by microporous membranes. the Third International Symposium on Progress in Membrane Science and Technology, Euromembrane, University of Twente.

Van der Graaf, S., Schroen, C., Boom, R. M. et al. (2005). "Preparation of double emulsions by membrane emulsification - a review." Journal of Membrane Science 251(1-2): 7-15.

Vladisavljevic, G. T. and Schubert, H. (2002). "Preparation and analysis of oil-in-water emulsions with a narrow droplet size distribution using Shirasu-porous-glass (SPG) membranes." Desalination 144(1-3): 167-172.

Vladisavljevic, G. T., Shimizu, M., et al. (2006). "Production of multiple emulsions for drug delivery systems by repeated SPG membrane homogenization: Influence of mean pore size, interfacial tension and continuous phase viscosity." Journal of Membrane Science 284(1-2): 373-383.

Vladisavljevic, G. T., Surh, J., et al. (2006). "Effect of emulsifier type on droplet disruption in repeated Shirasu porous glass membrane homogenization." Langmuir 22(10): 4526-4533.

Vladisavljevic, G. T. and Williams, R. A. (2005). "Recent developments in manufacturing emulsions and particulate products using membranes." Advances in Colloid and Interface Science 113(1): 1-20.

Vladisavljevic, G. T. and Williams R. A. (2006). "Manufacture of large uniform droplets using rotating membrane emulsification." Journal of Colloid and Interface Science 299(1): 396-402.

Wagdare, N. A., Marcelis, A., Ho, O. B., Boom, R. M., et al. (2010). "High throughput vegetable oil-in-water emulsification with a high porosity micro-engineered membrane." Journal of Membrane Science 347(1-2): 1-7.

Walstra, P. (1993). "Principles of emulsion formation." Chemical Engineering Science 48(2): 333-333.

Weiss, J., Decker, E. A., McClements, D. J., Kristbergsson, K., et al. (2008). "Solid lipid nanoparticles as delivery systems for bioactive food components." Food Biophys 3: 146-154.

Yuan, Q., Aryanti, N., et al. (2009). "Performance of slotted pores in particle manufacture using rotating membrane emulsification." Particuology 7(2): 114-120.

Yuan, Q., Williams, R. A., et al. (2010). "Innovations in high throughput manufacturing of uniform emulsions and capsules", Advanced Powder Technology 21(6): 599-608

Appendices

A   Droplet size and size distribution in the Span80/SDS system

The droplet size and size distribution were tested varying with the oscillation frequency under the same oscillation amplitude and preparation conditions, but different oil phase fluxes of $8.3\times10^{-6}\,\text{m}^3/(\text{m}^2\cdot\text{s})$, $13.8\times10^{-6}\text{m}^3/(\text{m}^2\cdot\text{s})$ and $19.4\times10^{-6}\text{m}^3/(\text{m}^2\cdot\text{s})$. The data are listed below.

Table A.1   The droplet size and size distribution as a function of oscillation frequency under different oil phase fluxes in the Span80/SDS system

Water=1000mL, SDS=1%w/v, Span80=4%w/v,
Amplitude=6mm, Flux=8.3×10^{-6}m^3/(m^2·s)

Frequency (Hz)	Sauter mean diameter (μm)	Coefficient of variation (%)
4.2	61.05	38
6.3	54.15	35
10.5	40.82	38
14.7	30.04	40
18.9	29.78	43

Water=1000mL, SDS=1%w/v, Span80=4%w/v,
Amplitude=6mm, Flux=13.8×10^{-6}m^3/(m^2·s)

Frequency (Hz)	Sauter mean diameter (μm)	Coefficient of variation (%)
6.3	59.40	42
8.4	47.68	33
10.5	42.79	35
14.7	34.13	37
18.9	32.33	38

Water=1000mL, SDS=1%w/v, Span80=4%w/v,
Amplitude=6mm, Flux=19.4×10^{-6}m^3/(m^2·s)

Frequency (Hz)	Sauter mean diameter (μm)	Coefficient of variation (%)
6.3	71.93	42
8.4	50.66	36
10.5	42.00	34
14.7	34.01	40
18.9	25.40	40

The droplet size and size distribution were tested varying with the oscillation frequency under the same oil phase flux and preparation conditions, but different oscillation amplitudes of 2mm, 6mm and 10mm. The data are listed below.

Table A.2   The droplet size and size distribution as a function of oscillation frequency under different amplitudes in the Span80/SDS system

Water=1000mL, SDS=1%w/v, Span80=4%w/v,
Flux=13.8×10^{-6}m^3/(m^2·s), amplitude=2mm

Frequency (Hz)	Sauter mean diameter (μm)	Coefficient of variation (%)
10.5	69.63	42
14.7	56.55	39
18.9	43.16	32
23.0	39.25	39

Water=1000mL, SDS=1%w/v, Span80=4%w/v,
Flux=13.8×10^{-6}m^3/(m^2·s), amplitude=6mm

Frequency (Hz)	Sauter mean diameter (μm)	Coefficient of variation (%)
6.3	59.40	42
8.4	47.68	33
10.5	42.79	35
14.7	34.13	37
18.9	32.33	38

Water=1000mL, SDS=1%w/v, Span80=4%w/v,
Flux=13.8×10^{-6}m^3/(m^2·s), amplitude=10mm

Frequency (Hz)	Sauter mean diameter (μm)	Coefficient of variation (%)
4.2	63.02	32
6.3	45.33	33
8.4	37.26	35
10.5	33.09	38
12.6	28.94	45

B   Droplet size and size distribution in the Span80/Tween20 system

The droplet size and size distribution were tested varying with the oscillation frequency under the same oil phase flux and preparation conditions, but different oscillation amplitudes of 2mm, 6mm and 10mm. The data are listed below.

Table B.1   The droplet size and size distribution as a function of oscillation frequency under different amplitudes in the Span80/Tween20 system

Water=1000mL, Tween20=4%w/v, Span80=4%w/v,
Flux=13.8×10^{-6}m^3/(m^2·s), amplitude=2mm

Frequency (Hz)	Sauter mean diameter (μm)	CV	Description
12.6	N/A	N/A	Severe coalescence. Oil layer formed on the water surface.
16.8	53.43	35	Coalescence on the membrane surface
20.9	50.43	37	No coalescence
25.1	47.71	36	No coalescence

75

Water=1000mL, Tween20=4%w/v, Span80=4%w/v, Flux=13.8×10^{-6}m^3/(m^2·s), amplitude=6mm			
Frequency (Hz)	Sauter mean diameter (μm)	CV	Description
8.4	57.35	49	Coalescence on the membrane surface
10.5	54.88	33	Slight coalescence on the membrane surface
12.6	43.47	35	No coalescence
14.7	42.60	35	No coalescence
18.9	37.93	33	No coalescence

Water=1000mL, Tween20=4%w/v, Span80=4%w/v, Flux=13.8×10^{-6}m^3/(m^2·s), amplitude=10mm			
Frequency (Hz)	Sauter mean diameter (μm)	CV	Description
6.3	53.47	54	Coalescence on the membrane surface
8.4	49.09	36	No coalescence
10.5	45.88	35	No coalescence
12.6	39.56	33	No coalescence

C Droplet size and size distribution in the continuous phase container with inserts

The width of continuous phase container was narrowed by attaching inserts on the both walls facing membranes. Three inserts with different surface geometries, such as the flat, the wavy and the surface with baffle plates, were investigated in the Span80/SDS system. The droplet size and size distribution were tested varying with the oscillation frequency under the same oil phase flux and preparation conditions, but different oscillation amplitudes of 2mm, 6mm and 10mm. The data are listed below.

Table C.1   The droplet size and size distribution as a function of oscillation frequency under different amplitudes in the container with flat inserts

Water=500mL, SDS=1%w/v, Span80=4%w/v,
Flux=13.8×10^{-6}m^3/(m^2·s), Amplitude=2mm, Flat inserts

Frequency (Hz)	Sauter mean diameter (μm)	Coefficient of variation (%)
10.5	47.42	53
14.7	37.73	48
18.9	31.54	43
23.0	27.38	45

Water=500mL, SDS=1%w/v, Span80=4%w/v,
Flux=13.8×10^{-6}m^3/(m^2·s), Amplitude=6mm, Flat inserts

Frequency (Hz)	Sauter mean diameter (μm)	Coefficient of variation (%)
6.3	44.11	43
8.4	38.47	41
10.5	32.32	45
14.7	29.28	48
18.9	27.76	49

Water=500mL, SDS=1%w/v, Span80=4%w/v,
Flux=13.8×10^{-6}m^3/(m^2·s), Amplitude=10mm, Flat inserts

Frequency (Hz)	Sauter mean diameter (μm)	Coefficient of variation (%)
4.2	49.16	37.5
6.3	39.82	38
8.4	33.67	39
10.5	28.81	45

Table C.2 The droplet size and size distribution as a function of oscillation frequency under different amplitudes in the container with wavy inserts

Water=500mL, SDS=1%w/v, Span80=4%w/v,
Flux=13.8×10^{-6}m^3/(m^2·s), Amplitude=2mm, Wavy inserts

Frequency (Hz)	Sauter mean diameter (μm)	Coefficient of variation (%)
10.5	51.87	47
14.7	38.57	45
18.9	30.12	42
23.0	27.13	47

Water=500mL, SDS=1%w/v, Span80=4%w/v,
Flux=13.8×10^{-6}m^3/(m^2·s), Amplitude=6mm, Wavy inserts

Frequency (Hz)	Sauter mean diameter (μm)	Coefficient of variation (%)
6.3	48.39	44
8.4	38.57	40
10.5	34.71	45
14.7	30.39	45.5
18.9	29.19	48

Water=500mL, SDS=1%w/v, Span80=4%w/v,
Flux=13.8×10^{-6}m^3/(m^2·s), Amplitude=10mm, Wavy inserts

Frequency (Hz)	Sauter mean diameter (μm)	Coefficient of variation (%)
4.2	53.09	37
6.3	41.39	39
8.4	32.96	42
10.5	31.57	43

Table C.3   The droplet size and size distribution as a function of oscillation frequency under different amplitudes in the container with baffles

Water=500mL, SDS=1%w/v, Span80=4%w/v,
Flux=13.8×10^{-6}m^3/(m^2·s), Amplitude=2mm, Baffle inserts

Frequency (Hz)	Sauter mean diameter (μm)	Coefficient of variation (%)
10.5	40.14	60.5
14.7	33.34	59
18.9	30.27	58
23	27.11	60

Water=500mL, SDS=1%w/v, Span80=4%w/v,
Flux=13.8×10^{-6}m^3/(m^2·s), Amplitude=6mm, Baffle inserts

Frequency (Hz)	Sauter mean diameter (μm)	Coefficient of variation (%)
6.3	39.72	52
8.4	36.81	46
10.5	31.53	52
14.7	25.78	52
18.9	21.91	52

Water=500mL, SDS=1%w/v, Span80=4%w/v,
Flux=13.8×10^{-6}m^3/(m^2·s), Amplitude=10mm, Baffle inserts

Frequency (Hz)	Sauter mean diameter (μm)	Coefficient of variation (%)
4.2	40.48	42
6.3	36.69	45
8.4	32.44	49
10.5	25.74	55

D   The measurement of interfacial tension

Table D.1   The list of interfacial tensions on the interfaces affected by different emulsifiers

Interface	Interfacial tension (mN/m)
Oil/Water	21.8760
Oil(4%w/v Span80)/Water(1%w/v SDS)	0.1969
Oil(4%w/v Span80)/Water(4%w/v Tween20)	0.2490
Oil(4%w/v Span80)/Water	0.6091
Oil/Water(4%w/v Tween20)	5.6620
Oil/Water(8%w/v Tween20)	5.1955

Curriculum Vitae

Name:	Jiangshan Liu
Post-secondary Education and Degrees:	The University of Western Ontario London, Ontario, Canada 2012-2013 M.E.Sc Beijing University of Chemical Technology Beijing, China 2008-2012 B.Eng
Honours and Awards:	Western Engineering Scholarship 2012-2013 Honors Graduate (Undergraduate) 2012 BASF Scholarship 2010-2011
Related Work Experience	Teaching Assistant The University of Western Ontario 2013 Research Assistant The University of Western Ontario 2012-2013

Publications:

- W. Zeng, H.G. Gomaa, J. Liu, J. Zhu, "Intensification of production of O/W emulsions using oscillatorywoven metal micro-screen (WMMS)", Chemical Engineering and Processing: Process Intensification, 2013 (Accepted)

- J. Liu, H.G. Gomaa, J. Zhu, "Oscillatory membrane emulsification" (to be submitted)